

# On Asymptotic Linear Convergence of Projected Gradient Descent for Constrained Least Squares

Trung Vu, *Graduate Student Member, IEEE*, Raviv Raich, *Senior Member, IEEE*

**Abstract**—Many recent problems in signal processing and machine learning such as compressed sensing, image restoration, matrix/tensor recovery, and non-negative matrix factorization can be cast as constrained optimization. Projected gradient descent is a simple yet efficient method for solving such constrained optimization problems. Local convergence analysis furthers our understanding of its asymptotic behavior near the solution, offering sharper bounds on the convergence rate compared to global convergence analysis. However, local guarantees often appear scattered in problem-specific areas of machine learning and signal processing. This manuscript presents a unified framework for the local convergence analysis of projected gradient descent in the context of constrained least squares. The proposed analysis offers insights into pivotal local convergence properties such as the condition of linear convergence, the region of convergence, the exact asymptotic rate of convergence, and the bound on the number of iterations needed to reach a certain level of accuracy. To demonstrate the applicability of the proposed approach, we present a recipe for the convergence analysis of PGD and demonstrate it via a beginning-to-end application of the recipe on four fundamental problems, namely, linearly constrained least squares, sparse recovery, least squares with the unit norm constraint, and matrix completion.

**Index Terms**—Projected gradient descent, constrained least squares, local convergence, asymptotic convergence rate.

## I. INTRODUCTION

CONSTRAINED least squares can be formulated as the following optimization problem:

$$\min_{\mathbf{x} \in \mathbb{R}^n} \frac{1}{2} \|\mathbf{A}\mathbf{x} - \mathbf{b}\|^2 \quad \text{s.t. } \mathbf{x} \in \mathcal{C}, \quad (1)$$

where  $\mathcal{C} \in \mathbb{R}^n$  is a non-empty closed set,  $\mathbf{A} \in \mathbb{R}^{m \times n}$ , and  $\mathbf{b} \in \mathbb{R}^m$  is the observation from which we wish to recover the solution  $\mathbf{x}^*$  efficiently. With the surge in the amount of data over the past decades, modern learning problems have become increasingly complex and optimization in the presence of constraints is frequently used to capture accurately their inherent structure. Examples in the area of machine learning and signal processing include, but are not limited to, compressed sensing [1]–[3], image restoration [4]–[6], seismic inversion [7]–[9], and phase-only beamforming [10], [11]. Since the set of real  $n_1 \times n_2$  matrices is isomorphic to  $\mathbb{R}^{n_1 n_2}$ , applications of (1) is also found in problems such as low-rank matrix recovery [12]–[14] and non-negative matrix factorization [15]–[17].

Projected gradient descent (PGD) is one of the most popular methods for solving constrained optimization, thanks to its simplicity and efficiency. In theory, convergence properties of

this method are natural extensions of the classical results for unconstrained optimization [18]–[21]. When the constraint set  $\mathcal{C}$  is convex, PGD is also known as the projected Landweber iteration [22] and is shown to converge sublinearly to the global solution of (1). Moreover, when the least-squares objective is strongly convex, the algorithm enjoys fast linear convergence. For non-convex settings, with the recent introduction of restricted (strong) convexity, global convergence has been guaranteed for certain structural constraints such as sparsity constraint [23], low-rank constraint [24], and L2-norm constraint [25].

From a different perspective, problem (1) can be viewed as a manifold optimization problem in which the intrinsic structure of manifolds can be exploited. Dating back to the 1970s, Luenberger [26] studied a variant of gradient projection method using the concept of geodesic descent. Under the assumption that  $\mathcal{C}$  is a differentiable manifold in Euclidean space, the author provided sufficient conditions for global convergence and established a sharp bound on the asymptotic convergence rate near a strict local minimum. Later on, this result was extended to a broader class of Riemannian manifolds and has been widely known as the Riemannian steepest descent method [27]–[29]. The asymptotic convergence rate of Riemannian steepest descent (with exact line search) is given by the Kantorovich ratio  $(\beta - \alpha)^2 / (\beta + \alpha)^2$ , where  $\alpha$  and  $\beta$  are the smallest and largest eigenvalues of the second derivative of the Lagrangian restricted to the subspace tangent to the constraint manifold at the solution. Remarkably, such local convergence bounds are tighter than those obtained from the aforementioned global convergence analysis in the optimization literature since the former exploits the local structure of the problem. The global convergence bounds, on the other hand, take into account the worst-case behavior of the algorithm that might occur far away from the solution of interest. In certain situations, global convergence analysis suggests sublinear convergence while local convergence analysis offers linear convergence thanks to the benign structure near the solution [30].

One key element in the asymptotic convergence analysis of Riemannian steepest descent is Kantorovich inequality [31]. However, this technique depends on the optimal choice of step size in the exact line search scheme and is not straightforwardly generalized to other variants of gradient projection. In particular, to the best of our knowledge, there has been no direct extension of the analysis for Riemannian steepest descent method [26]–[28] to plain PGD with a fixed step size. In this manuscript, we employ a different technique to analyze the asymptotic convergence of PGD with a fixed

Trung Vu and Raviv Raich are with the School of Electrical Engineering and Computer Science, Oregon State University, Corvallis, OR 97331, USA. (e-mails: vutru@oregonstate.edu and raich@oregonstate.edu).

step size. Our technique relies on two key factors: (i) the approximation of the projection operator near the solution and (ii) the convergence of the asymptotically-linear quadratic difference equation on the error through iterations. This enables us to develop a unified framework for local convergence analysis of PGD for solving (1), generalizing our previous work in [32]–[36]. The proposed framework is the first to offer sufficient conditions for local linear convergence, a closed-form expression of the exact asymptotic rate of convergence, and the bound on the number of iterations needed to reach a certain level of accuracy. As a demonstration, we present the application of our framework to four well-known problems in machine learning and signal processing, namely, linearly constrained least squares, sparse recovery, least squares with spherical constraint, and matrix completion. We show that the obtained asymptotic rate of convergence matches existing results in the literature. For problems in which the exact convergence rate of PGD has not been studied, we verify the asymptotic rate obtained by our analysis against the rate of convergence obtained in numerical experiments. Beyond these examples, our proposed framework can be used as a general recipe to develop quick yet sharp convergence results for PGD in other applications in the field.

## II. NOTATIONS

Throughout the paper, we use the notation  $\|\cdot\|$  to denote the Euclidean norm. In a more specific context,  $\|\cdot\|_F$  and  $\|\cdot\|_2$  denote the Frobenius norm and the spectral norm of a matrix, respectively. Boldfaced symbols are reserved for vectors and matrices. Additionally, the  $t \times t$  identity matrix is denoted by  $\mathbf{I}_t$  and the  $i$ th vector in the natural basis of  $\mathbb{R}^n$  is denoted by  $\mathbf{e}_i$ .  $\otimes$  represents the Kronecker product between two matrices.  $\text{vec}(\cdot)$  denotes the vectorization of a matrix by stacking its columns on top of one another. Given  $\mathbf{x} \in \mathbb{R}^n$ ,  $\text{diag}(\mathbf{x})$  denotes the diagonal matrix with diagonal entries are the  $n$  elements of  $\mathbf{x}$ . For a scalar  $r > 0$ , denote the open ball of center  $\mathbf{x}$  and radius  $r$  by  $\mathcal{B}(\mathbf{x}, r) = \{\mathbf{y} \mid \|\mathbf{y} - \mathbf{x}\| < r\}$ . Correspondingly, the closed ball of center  $\mathbf{x}$  and radius  $r$  is denoted by  $\mathcal{B}[\mathbf{x}, r] = \{\mathbf{y} \mid \|\mathbf{y} - \mathbf{x}\| \leq r\}$ . Division by zero is defined as  $a/0 = \infty$  for  $a \neq 0$ , with the sign matching that of  $a$ . The lexicographical order between two vectors  $\mathbf{x}$  and  $\mathbf{y}$  of the same length is defined by  $\mathbf{x} < \mathbf{y}$  if  $x_i < y_i$  for the first  $i$  ( $i$  goes from 1) where  $x_i$  and  $y_i$  differs. The lexicographical order between two matrices  $\mathbf{X}$  and  $\mathbf{Y}$  of the same size is define by the lexicographical order between  $\text{vec}(\mathbf{X})$  and  $\text{vec}(\mathbf{Y})$ .

Given  $\mathbf{A} \in \mathbb{R}^{m \times n}$ , the  $i$ th largest eigenvalue and the  $i$ th largest singular value of  $\mathbf{A}$  are denoted by  $\lambda_i(\mathbf{A})$  and  $\sigma_i(\mathbf{A})$ , respectively. The spectral radius of  $\mathbf{A}$  is defined as  $\rho(\mathbf{A}) = \max_i |\lambda_i(\mathbf{A})|$ . Gelfand's formula [37] states that  $\rho(\mathbf{A}) = \lim_{k \rightarrow \infty} \|\mathbf{A}^k\|_2^{1/k} \leq \|\mathbf{A}\|_2$ . If  $\mathbf{A}$  is square and invertible, the condition number of  $\mathbf{A}$  is defined as  $\kappa(\mathbf{A}) = \sigma_1(\mathbf{A})/\sigma_n(\mathbf{A})$ .

## III. PRELIMINARIES

This section presents some key concepts and results that will be used as the basic premise of our convergence analysis.

### A. Nonlinear Orthogonal Projections

Given a non-empty set  $\mathcal{C} \subset \mathbb{R}^n$ , let us define the distance from a point  $\mathbf{x} \in \mathbb{R}^n$  to  $\mathcal{C}$  as

$$d(\mathbf{x}, \mathcal{C}) = \inf_{\mathbf{y} \in \mathcal{C}} \{\|\mathbf{y} - \mathbf{x}\|\}. \quad (2)$$

The set of all projections of  $\mathbf{x}$  onto  $\mathcal{C}$  is defined by

$$\Pi_{\mathcal{C}}(\mathbf{x}) = \{\mathbf{y} \in \mathcal{C} \mid \|\mathbf{y} - \mathbf{x}\| = d(\mathbf{x}, \mathcal{C})\}. \quad (3)$$

It is well-known [38] that if  $\mathcal{C}$  is closed, then for any  $\mathbf{x} \in \mathbb{R}^n$ ,  $\Pi_{\mathcal{C}}(\mathbf{x})$  is non-empty<sup>1</sup>. An orthogonal projection onto  $\mathcal{C}$  is defined as  $\mathcal{P}_{\mathcal{C}} : \mathbb{R}^n \rightarrow \mathcal{C}$  such that  $\mathcal{P}_{\mathcal{C}}(\mathbf{x})$  is chosen as an element of  $\Pi_{\mathcal{C}}(\mathbf{x})$  based on a prescribed scheme (e.g., based on lexicographic order).

**Definition 1.** *Let*

$$\text{dom } \mathcal{P}_{\mathcal{C}} = \{\mathbf{x} \in \mathbb{R}^n \mid \Pi_{\mathcal{C}}(\mathbf{x}) \text{ is singleton}\}.$$

$\mathcal{P}_{\mathcal{C}}$  is said to be **differentiable** at  $\mathbf{x} \in \text{dom } \mathcal{P}_{\mathcal{C}}$  if there exists  $\nabla \mathcal{P}_{\mathcal{C}}(\mathbf{x}) \in \mathbb{R}^{n \times n}$  such that

$$\lim_{\delta \rightarrow \mathbf{0}} \sup_{\mathbf{y} \in \Pi_{\mathcal{C}}(\mathbf{x} + \delta)} \frac{\|\mathbf{y} - \mathcal{P}_{\mathcal{C}}(\mathbf{x}) - \nabla \mathcal{P}_{\mathcal{C}}(\mathbf{x})\delta\|}{\|\delta\|} = 0.$$

The operator  $\nabla \mathcal{P}_{\mathcal{C}}(\mathbf{x})$  is called the derivative of  $\mathcal{P}_{\mathcal{C}}$  at  $\mathbf{x}$ . In addition,  $\mathcal{P}_{\mathcal{C}}$  is said to be **Lipschitz-continuously differentiable** at  $\mathbf{x}$  if there exist  $0 < c_1(\mathbf{x}) \leq \infty$  and  $0 \leq c_2(\mathbf{x}) < \infty$  such that for any  $\delta \in \mathcal{B}(\mathbf{0}, c_1(\mathbf{x}))$ , we have

$$\sup_{\mathbf{y} \in \Pi_{\mathcal{C}}(\mathbf{x} + \delta)} \|\mathbf{y} - \mathcal{P}_{\mathcal{C}}(\mathbf{x}) - \nabla \mathcal{P}_{\mathcal{C}}(\mathbf{x})\delta\| \leq c_2(\mathbf{x})\|\delta\|^2. \quad (4)$$

It is noted that the supremum in (4) implies

$$\|\mathcal{P}_{\mathcal{C}}(\mathbf{x} + \delta) - \mathcal{P}_{\mathcal{C}}(\mathbf{x}) - \nabla \mathcal{P}_{\mathcal{C}}(\mathbf{x})\delta\| \leq c_2(\mathbf{x})\|\delta\|^2$$

holds for any choice of  $\mathcal{P}_{\mathcal{C}}(\mathbf{x} + \delta)$ . Generally, if  $\mathcal{P}_{\mathcal{C}}$  is of class  $C^1$ , then it is differentiable at every  $\mathbf{x} \in \text{dom } \mathcal{P}_{\mathcal{C}}$  but not necessarily Lipschitz-continuously differentiable at  $\mathbf{x}$ . On the other hand,  $\mathcal{P}_{\mathcal{C}}$  is  $C^2$  ensures  $\mathcal{P}_{\mathcal{C}}$  is Lipschitz-continuously differentiable at every  $\mathbf{x} \in \text{dom } \mathcal{P}_{\mathcal{C}}$  but the vice versa does not always hold.

**Example 1.** *Let  $\mathcal{C} = \{\mathbf{x} \in \mathbb{R}^n \mid \|\mathbf{x}\| = 1\}$  be the unit sphere of dimension  $n - 1$ . For any  $\mathbf{x} \neq \mathbf{0}$ , the projection onto  $\mathcal{C}$  is uniquely given by  $\mathcal{P}_{\mathcal{C}}(\mathbf{x}) = \mathbf{x}/\|\mathbf{x}\|$ . For  $\mathbf{x} = \mathbf{0}$ , we have  $\Pi_{\mathcal{C}}(\mathbf{0}) = \mathcal{C}$  and  $\mathcal{P}_{\mathcal{C}}(\mathbf{0})$  can be chosen as any point on the unit sphere. In Appendix A, we prove that  $\mathcal{P}_{\mathcal{C}}$  is Lipschitz-continuously differentiable in  $\text{dom } \mathcal{P}_{\mathcal{C}} = \mathbb{R}^n \setminus \{\mathbf{0}\}$ . In particular, for any  $\mathbf{x} \neq \mathbf{0}$  and  $\delta \in \mathbb{R}^n$ , we have*

$$\sup_{\mathbf{y} \in \Pi_{\mathcal{C}}(\mathbf{x} + \delta)} \left\| \mathbf{y} - \frac{\mathbf{x}}{\|\mathbf{x}\|} - \left( \mathbf{I}_n - \frac{\mathbf{x}\mathbf{x}^\top}{\|\mathbf{x}\|^2} \right) \frac{\delta}{\|\mathbf{x}\|} \right\| \leq \frac{2}{\|\mathbf{x}\|^2} \|\delta\|^2. \quad (5)$$

For  $\delta \neq -\mathbf{x}$ ,  $\Pi_{\mathcal{C}}(\mathbf{x} + \delta) = \{(\mathbf{x} + \delta)/\|\mathbf{x} + \delta\|\}$  is singleton and the supremum is evaluated at only one point  $\mathbf{y} = (\mathbf{x} + \delta)/\|\mathbf{x} + \delta\|$ . For  $\delta = -\mathbf{x}$ , the supremum is taken over the entire sphere independent of  $\mathbf{x}$ . By Definition 1, we obtain

$$\begin{aligned} \nabla \mathcal{P}_{\mathcal{C}}(\mathbf{x}) &= \frac{1}{\|\mathbf{x}\|} \left( \mathbf{I}_n - \frac{\mathbf{x}\mathbf{x}^\top}{\|\mathbf{x}\|^2} \right), \\ c_1(\mathbf{x}) &= \infty, \quad c_2(\mathbf{x}) = \frac{2}{\|\mathbf{x}\|^2}. \end{aligned}$$

<sup>1</sup>In addition, if  $\mathcal{C}$  is convex, then  $\Pi_{\mathcal{C}}(\mathbf{x})$  is singleton.

**Algorithm 1** Projected Gradient Descent (PGD)**Input:**  $f, \mathcal{C}, \eta, \mathbf{x}^{(0)}$ **Output:**  $\{\mathbf{x}^{(k)}\}$ 

1: **for**  $k = 0, 1, \dots$  **do**  
 2:  $\mathbf{x}^{(k+1)} = \mathcal{P}_{\mathcal{C}}(\mathbf{x}^{(k)} - \eta \mathbf{A}^\top(\mathbf{A}\mathbf{x}^{(k)} - \mathbf{b}))$

In 1984, Foote [39] showed that if  $\mathcal{C}$  is a  $C^k$  ( $k \geq 2$ ) submanifold of  $\mathbb{R}^n$ , then  $\mathcal{C}$  has a neighborhood  $\mathcal{E}$  such that  $\mathcal{E} \subseteq \text{dom } \mathcal{P}_{\mathcal{C}}$  and the projection  $\mathcal{P}_{\mathcal{C}}$  restricted to  $\mathcal{E}$  is a  $C^{k-1}$  mapping. Later on, Dudek and Holly [40] proved the derivative  $\nabla \mathcal{P}_{\mathcal{C}}$  is a linear map to the tangent bundle of  $\mathcal{C}$  and more importantly, for any  $\mathbf{x}^* \in \mathcal{C}$ ,  $\nabla \mathcal{P}_{\mathcal{C}}(\mathbf{x}^*)$  is the (linear) orthogonal projection onto the tangent space to  $\mathcal{C}$  at  $\mathbf{x}^*$ . Recently, a local version of this result has been proposed by Lewis and Malick [41]:

**Proposition 1.** (Rephrased from Lemma 4 in [41]) Assume  $\mathcal{C}$  is a  $C^k$  ( $k \geq 2$ ) manifold around a point  $\mathbf{x}^* \in \mathcal{C}$ . Denote the tangent space to  $\mathcal{C}$  at  $\mathbf{x}^*$  by  $T_{\mathbf{x}^*}(\mathcal{C})$ . Then,  $\mathcal{P}_{\mathcal{C}}$  is a  $C^{k-1}$  mapping around  $\mathbf{x}^*$  and

$$\nabla \mathcal{P}_{\mathcal{C}}(\mathbf{x}^*) = \mathcal{P}_{T_{\mathbf{x}^*}(\mathcal{C})}, \quad (6)$$

where  $\mathcal{P}_{T_{\mathbf{x}^*}(\mathcal{C})}$  is the orthogonal projection onto  $T_{\mathbf{x}^*}(\mathcal{C})$ .

Further works on the uniqueness and regularity of  $\mathcal{P}_{\mathcal{C}}$  can also be found in [42]–[45]. We note that the assumption  $\mathcal{C}$  is a  $C^2$  manifold around  $\mathbf{x}^*$  requires the existence of a neighborhood of  $\mathbf{x}^*$  in which  $\mathcal{P}_{\mathcal{C}}$  is uniformly differentiable. Our result in this manuscript, while strongly motivated by the aforementioned results, only requires  $\mathcal{C}$  to be differentiable at two points (see Theorem 1).

### B. Stationary Points

We defined the (Lipschitz-continuous) differentiability of the projection  $\mathcal{P}_{\mathcal{C}}$  at a point in  $\mathcal{C}$ . We are now in position to define stationary points of (1) as those where the gradient of the objective function on the constraint set vanishes [46]:

**Definition 2.**  $\mathbf{x}^* \in \mathcal{C}$  is a **stationary point** of (1) if  $\mathcal{P}_{\mathcal{C}}$  is differentiable at  $\mathbf{x}^*$  and

$$\nabla \mathcal{P}_{\mathcal{C}}(\mathbf{x}^*) \cdot \mathbf{A}^\top(\mathbf{A}\mathbf{x}^* - \mathbf{b}) = \mathbf{0}. \quad (7)$$

Assume in addition that  $\mathcal{P}_{\mathcal{C}}$  is Lipschitz-continuously differentiable at  $\mathbf{x}^*$  with constants  $c_1(\mathbf{x}^*)$  and  $c_2(\mathbf{x}^*)$ . Then  $\mathbf{x}^*$  is called a **Lipschitz stationary point** of (1) with constants  $c_1(\mathbf{x}^*)$  and  $c_2(\mathbf{x}^*)$ .

Similar to unconstrained optimization, stationary points in Definition 2 can be local minimizers, local maximizers, or saddle points of the constrained problem (1).

### C. Projected Gradient Descent

Algorithm 1 describes the projected gradient descent algorithm for solving (1). Starting at some  $\mathbf{x}^{(0)} \in \mathcal{C}$ , the algorithm iteratively updates the current value by (i) taking a step in the

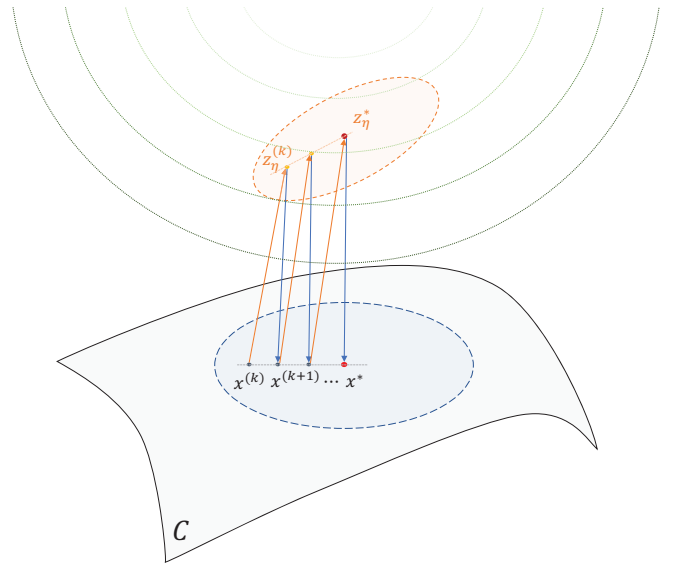


Fig. 1: Illustration of convergence of projected gradient descent to a fixed point  $\mathbf{x}^*$ . In order to guarantee linear convergence, Theorem 1 requires  $\mathcal{P}_{\mathcal{C}}$  to be Lipschitz-continuously differentiable at both  $\mathbf{x}^{(k)}$  and  $\mathbf{z}_\eta^* = \mathbf{x}^{(k)} - \eta \mathbf{A}^\top(\mathbf{A}\mathbf{x}^{(k)} - \mathbf{b})$ . Moreover, the condition  $\|\mathbf{x}^{(0)} - \mathbf{x}^*\| < \min\{c_1(\mathbf{x}^*)/\kappa(\mathbf{Q}), c_1(\mathbf{z}_\eta^*)/(\kappa(\mathbf{Q})u_\eta)\}$  from (12) ensures that remains inside  $\mathcal{B}(\mathbf{x}^*, c_1(\mathbf{x}^*))$  (blue dashed ellipse) and  $\mathbf{z}_\eta^* = \mathbf{x}^{(k)} - \eta \mathbf{A}^\top(\mathbf{A}\mathbf{x}^{(k)} - \mathbf{b})$  remains inside  $\mathcal{B}(\mathbf{z}_\eta^*, c_1(\mathbf{z}_\eta^*))$  (orange dashed ellipse).

opposite direction of the gradient and (ii) projecting the result back onto  $\mathcal{C}$ , i.e.,

$$\mathbf{x}^{(k+1)} = \mathcal{P}_{\mathcal{C}}(\mathbf{x}^{(k)} - \eta \mathbf{A}^\top(\mathbf{A}\mathbf{x}^{(k)} - \mathbf{b})), \quad (8)$$

where  $\eta > 0$  is a fixed step size.

**Definition 3.**  $\mathbf{x}^*$  is a **fixed point** of Algorithm 1 with step size  $\eta > 0$  if

$$\mathbf{x}^* = \mathcal{P}_{\mathcal{C}}(\mathbf{x}^* - \eta \mathbf{A}^\top(\mathbf{A}\mathbf{x}^* - \mathbf{b})). \quad (9)$$

**Lemma 1.** If  $\mathbf{x}^*$  is a fixed point of Algorithm 1 with some step size  $\eta > 0$  and  $\mathcal{P}_{\mathcal{C}}$  is differentiable at  $\mathbf{x}^*$ , then  $\mathbf{x}^*$  is a stationary point of (1).

The proof of Lemma 1 is given in Appendix B.

## IV. LOCAL CONVERGENCE ANALYSIS

In this section, we present our local convergence analysis of projected gradient descent for constrained least squares. Figure 1 illustrates the key idea in our analysis. In order to establish the local linear convergence of Algorithm 1 to its fixed point  $\mathbf{x}^*$ , we require the Lipschitz-continuous differentiability of  $\mathcal{P}_{\mathcal{C}}$  at  $\mathbf{x}^*$  and at  $\mathbf{z}_\eta^* = \mathbf{x}^* - \eta \mathbf{A}^\top(\mathbf{A}\mathbf{x}^* - \mathbf{b})$ . These properties enables us to approximate each projected gradient descent update by a linear operator on the error vector (i.e., the difference between  $\mathbf{x}^{(k)}$  and  $\mathbf{x}^*$ ). Then, under the additional assumption that this linear operator is a contraction mapping and the initialization  $\mathbf{x}^{(0)}$  is sufficiently close to  $\mathbf{x}^*$ , we show that the gradient step and the projection step remain inside the Lipschitz-continuous differentiability regions of  $\mathbf{x}^*$  (i.e.,  $\mathcal{B}(\mathbf{x}^*, c_1(\mathbf{x}^*))$ ) and  $\mathbf{z}_\eta^*$  (i.e.,  $\mathcal{B}(\mathbf{z}_\eta^*, c_1(\mathbf{z}_\eta^*))$ ), respectively.

### A. Main Results

In this following, we state our main result in Theorem 1, followed by further insights into the convergence results.

**Theorem 1.** *Suppose  $\mathbf{x}^*$  is a fixed point of Algorithm 1 with step size  $\eta > 0$  such that the following conditions hold:*

- 1)  $\mathcal{P}_C$  is Lipschitz-continuously differentiable at both the fixed point  $\mathbf{x}^*$  and at the gradient step taken from the fixed point

$$\mathbf{z}_\eta^* = \mathbf{x}^* - \eta \mathbf{A}^\top (\mathbf{A} \mathbf{x}^* - \mathbf{b}), \quad (10)$$

with the corresponding matrices  $\nabla \mathcal{P}_C(\mathbf{x}^*)$ ,  $\nabla \mathcal{P}_C(\mathbf{z}_\eta^*)$ , and constants  $c_1(\mathbf{x}^*)$ ,  $c_2(\mathbf{x}^*)$ ,  $c_1(\mathbf{z}_\eta^*)$ , and  $c_2(\mathbf{z}_\eta^*)$ .

- 2) The matrix

$$\mathbf{H} = \nabla \mathcal{P}_C(\mathbf{z}_\eta^*) (\mathbf{I}_n - \eta \mathbf{A}^\top \mathbf{A}) \nabla \mathcal{P}_C(\mathbf{x}^*) \quad (11)$$

admits an eigendecomposition  $\mathbf{H} = \mathbf{Q} \mathbf{\Lambda} \mathbf{Q}^{-1}$ , where  $\mathbf{Q} \in \mathbb{R}^{n \times n}$  is an invertible matrix and  $\mathbf{\Lambda}$  is a diagonal matrix whose diagonal entries are strictly less than 1 in magnitude, i.e.,  $\rho(\mathbf{H}) = \|\mathbf{\Lambda}\|_2 < 1$ .

- 3) The initial iterate  $\mathbf{x}^{(0)}$  satisfies

$$\|\mathbf{x}^{(0)} - \mathbf{x}^*\| < \min \left\{ \frac{c_1(\mathbf{x}^*)}{\kappa(\mathbf{Q})}, \frac{c_1(\mathbf{z}_\eta^*)}{\kappa(\mathbf{Q}) u_\eta}, \frac{1 - \rho(\mathbf{H})}{q} \right\}, \quad (12)$$

where

$$u_\eta = \|\mathbf{I}_n - \eta \mathbf{A}^\top \mathbf{A}\|_2 \quad (13)$$

and

$$q = \kappa^2(\mathbf{Q}) u_\eta (c_2(\mathbf{z}_\eta^*) u_\eta + \|\nabla \mathcal{P}_C(\mathbf{z}_\eta^*)\|_2 c_2(\mathbf{x}^*)). \quad (14)$$

Let  $\{\mathbf{x}^{(k)}\}_{k=0}^\infty$  be the vector sequence generated by the PGD update in (8). Then, for any  $0 < \epsilon < 1$ , we have  $\|\mathbf{x}^{(k)} - \mathbf{x}^*\| \leq \epsilon \|\mathbf{x}^{(0)} - \mathbf{x}^*\|$  for all

$$k \geq \frac{\log(1/\epsilon) + \log(\kappa(\mathbf{Q}))}{\log(1/\rho(\mathbf{H}))} + c_3, \quad (15)$$

where  $c_3 > 0$ , given explicitly in Lemma 4, is independent of  $\epsilon$ . Algorithm 1 is said to converge locally to  $\mathbf{x}^*$  at an **asymptotic linear rate**  $\rho(\mathbf{H})$  with the **region of linear convergence** given by (12).

Theorem 1 states the sufficient conditions for asymptotic linear convergence of Algorithm 1. In addition, the theorem establishes the asymptotic rate as the spectral radius of the matrix  $\mathbf{H}$  and bounds the number of iterations needed to reach  $\epsilon$ -accuracy. The proof of Theorem 1 is given in Subsection IV-B. It is noteworthy that in the RHS of (15), the first term corresponds to linear convergence in the asymptotic regime and the second term corresponds to nonlinear convergence behavior at the early stage. We will revisit this point when we introduce Lemma 4.

**Remark 1.** When  $\mathbf{H}$  is symmetric, its eigendecomposition exists and can be represented as

$$\mathbf{H} = \mathbf{Q} \mathbf{\Lambda} \mathbf{Q}^\top,$$

where  $\mathbf{Q}$  is an orthogonal matrix with  $\kappa(\mathbf{Q}) = 1$ .

Next, we study a special case of Theorem 1 in which

$$\nabla \mathcal{P}_C(\mathbf{z}_\eta^*) = \nabla \mathcal{P}_C(\mathbf{x}^*) = \mathcal{P}_{T_{\mathbf{x}^*}(\mathcal{C})} = \mathbf{U}_{\mathbf{x}^*} \mathbf{U}_{\mathbf{x}^*}^\top, \quad (16)$$

where  $\mathbf{U}_{\mathbf{x}^*} \in \mathbb{R}^{n \times d}$  ( $d \leq n$ ) is the matrix whose columns provide an orthonormal basis for the tangent space to  $\mathcal{C}$  at  $\mathbf{x}^*$ . A typical example in which (16) holds is when (i)  $\mathcal{C}$  is a  $C^2$   $d$ -dimensional submanifold around  $\mathbf{x}^*$ ; and (ii)  $\mathbf{z}_\eta^* = \mathbf{x}^*$ . The first condition (i) stems from Proposition 1 in order to guarantee  $\nabla \mathcal{P}_C(\mathbf{x}^*) = \mathcal{P}_{T_{\mathbf{x}^*}(\mathcal{C})}$ . The second condition (ii) is equivalent to  $\mathbf{A}^\top (\mathbf{A} \mathbf{x} - \mathbf{b}) = \mathbf{0}$ , which means  $\mathbf{x}^*$  is also a stationary point of the unconstrained problem. Conveniently, this coincidence eliminates the task of characterizing the projection  $\mathcal{P}_C$  and its derivative  $\nabla \mathcal{P}_C$  at a point outside  $\mathcal{C}$ , which can be a challenging task in many problems.

**Corollary 1.** *Consider the same setting as in Theorem 1 with the additional assumption that (16) holds. If  $(\mathbf{A} \mathbf{U}_{\mathbf{x}^*})^\top \mathbf{A} \mathbf{U}_{\mathbf{x}^*}$  has full rank and*

$$0 < \eta < \frac{2}{\|\mathbf{A} \mathbf{U}_{\mathbf{x}^*}\|_2^2}, \quad (17)$$

then Algorithm 1 with fixed step size  $\eta$  converges locally to  $\mathbf{x}^*$  at an asymptotic linear rate

$$\rho(\mathbf{H}) = \max\{|1 - \eta \lambda_1|, |1 - \eta \lambda_d|\}, \quad (18)$$

where  $\lambda_1$  and  $\lambda_d$  are the largest and smallest eigenvalues of  $(\mathbf{A} \mathbf{U}_{\mathbf{x}^*})^\top \mathbf{A} \mathbf{U}_{\mathbf{x}^*}$ , respectively. The region of linear convergence is given by

$$\|\mathbf{x}^{(0)} - \mathbf{x}^*\| < \min \left\{ c_1(\mathbf{x}^*), \frac{c_1(\mathbf{z}_\eta^*)}{u_\eta}, \frac{1 - \rho(\mathbf{H})}{u_\eta c_2(\mathbf{x}^*) + u_\eta^2 c_2(\mathbf{z}_\eta^*)} \right\}, \quad (19)$$

where  $u_\eta$  is given by (13).

The proof of Corollary 1 is given in Appendix C.

**Remark 2.** Recall that  $u_\eta$  defined in (13) is also the asymptotic linear rate of gradient descent for the unconstrained least squares [47], i.e.,

$$u_\eta = \max\{|1 - \eta \lambda_1(\mathbf{A}^\top \mathbf{A})|, |1 - \eta \lambda_n(\mathbf{A}^\top \mathbf{A})|\}.$$

Since  $\mathbf{U}_{\mathbf{x}^*}$  is a semi-orthogonal matrix, the eigenvalues of  $\mathbf{U}_{\mathbf{x}^*}^\top \mathbf{A}^\top \mathbf{A} \mathbf{U}_{\mathbf{x}^*}$  interlace with those of  $\mathbf{A}^\top \mathbf{A}$  [48], which in turns implies

$$\lambda_n(\mathbf{A}^\top \mathbf{A}) \leq \lambda_d \leq \lambda_1 \leq \lambda_1(\mathbf{A}^\top \mathbf{A}).$$

Thus, one can show that for  $\eta < 2/\|\mathbf{A}\|_2^2$ ,

$$\rho(\mathbf{H}) \leq u_\eta \leq 1, \quad (20)$$

with the equality  $u_\eta = 1$  holding if and only if  $\mathbf{A}^\top \mathbf{A}$  is singular. Interestingly, (20) implies the presence of the constraint in this case helps accelerate the convergence of gradient descent to  $\mathbf{x}^*$ .

### B. Proof of Theorem 1

This section presents the proof of Theorem 1. Our key ideas are: **(1)** using the Lipschitz-continuous differentiability of  $\mathcal{P}_C$  at  $\mathbf{x}^*$  and at  $\mathbf{z}_\eta^*$  to establish a recursive relation on the error vector  $\boldsymbol{\delta}^{(k)} = \mathbf{x}^{(k)} - \mathbf{x}^*$ , **(2)** performing a change of basis  $\tilde{\boldsymbol{\delta}}^{(k)} = \mathbf{Q}^{-1}\boldsymbol{\delta}^{(k)}$  to establish an asymptotically-linear quadratic system dynamic that upper-bounds the norm of the transformed error vector, **(3)** applying the result on the convergence of an asymptotically-linear quadratic difference equation in [49] to obtain the number of iterations required for  $\|\tilde{\boldsymbol{\delta}}^{(k)}\| \leq \tilde{\epsilon}\|\tilde{\boldsymbol{\delta}}^{(0)}\|$ , and **(4)** converting the convergence result on the transformed error  $\|\tilde{\boldsymbol{\delta}}^{(k)}\|$  to the convergence result on the original error  $\|\boldsymbol{\delta}^{(k)}\|$ . In the following, we provide the complete proof, with some details deferred to the appendix.

**Step 1:** Let us define the error vector of Algorithm 1 as  $\boldsymbol{\delta}^{(k)} = \mathbf{x}^{(k)} - \mathbf{x}^*$ , for  $k \in \mathbb{N}$ . Using this definition of the error vector, we can replace  $\mathbf{x}^{(k)} = \mathbf{x}^* + \boldsymbol{\delta}^{(k)}$  and  $\mathbf{x}^{(k+1)} = \mathbf{x}^* + \boldsymbol{\delta}^{(k+1)}$  into (8) to obtain an equivalent update on the error vector

$$\boldsymbol{\delta}^{(k+1)} = \mathcal{P}_C\left(\mathbf{x}^* + \boldsymbol{\delta}^{(k)} - \eta\mathbf{A}^\top(\mathbf{A}(\mathbf{x}^* + \boldsymbol{\delta}^{(k)}) - \mathbf{b})\right) - \mathbf{x}^*. \quad (21)$$

Based on the definition of  $\mathbf{z}_\eta^*$  in (10) and the fact that  $\mathbf{x}^*$  is a fixed point of the algorithm (see (9)), i.e.,  $\mathbf{x}^* = \mathcal{P}_C(\mathbf{z}_\eta^*)$ , we can rewrite (21) as

$$\boldsymbol{\delta}^{(k+1)} = \mathcal{P}_C\left(\mathbf{z}_\eta^* + (\mathbf{I} - \eta\mathbf{A}^\top\mathbf{A})\boldsymbol{\delta}^{(k)}\right) - \mathcal{P}_C(\mathbf{z}_\eta^*). \quad (22)$$

We are now in position to analyze the error update as a fixed-point iteration:  $\boldsymbol{\delta}^{(k+1)} = \mathbf{f}(\boldsymbol{\delta}^{(k)})$ , where  $\mathbf{f}(\boldsymbol{\delta}) = \mathcal{P}_C(\mathbf{z}_\eta^* + (\mathbf{I} - \eta\mathbf{A}^\top\mathbf{A})\boldsymbol{\delta}) - \mathcal{P}_C(\mathbf{z}_\eta^*)$ . The following lemma provides a recursive equation on the error vector that is in the form of an asymptotically-linear quadratic system dynamic:

**Lemma 2.** Recall  $\mathbf{H} = \nabla\mathcal{P}_C(\mathbf{z}_\eta^*)(\mathbf{I}_n - \eta\mathbf{A}^\top\mathbf{A})\nabla\mathcal{P}_C(\mathbf{x}^*)$ . If the error vector at the  $k$ -th iteration satisfies

$$\|\boldsymbol{\delta}^{(k)}\| < \min\left\{c_1(\mathbf{x}^*), \frac{c_1(\mathbf{z}_\eta^*)}{u_\eta}\right\}, \quad (23)$$

then the error vector at the  $k+1$ -th iteration satisfies

$$\boldsymbol{\delta}^{(k+1)} = \mathbf{H}\boldsymbol{\delta}^{(k)} + \mathbf{q}_2(\boldsymbol{\delta}^{(k)}), \quad (24)$$

where  $\mathbf{q}_2: \mathbb{R}^n \rightarrow \mathbb{R}^n$  is the residual such that

$$\|\mathbf{q}_2(\boldsymbol{\delta}^{(k)})\| \leq (\|\nabla\mathcal{P}_C(\mathbf{z}_\eta^*)\|_2 u_\eta c_2(\mathbf{x}^*) + c_2(\mathbf{z}_\eta^*) u_\eta^2) \|\boldsymbol{\delta}^{(k)}\|^2. \quad (25)$$

The detailed proof of Lemma 2 is given in Appendix D.

**Remark 3.** In [50], Polyak studied the convergence of non-linear difference equations of form

$$\mathbf{a}^{(k+1)} = \mathbf{T}(\mathbf{a}^{(k)}) + \mathbf{q}(\mathbf{a}^{(k)}), \quad \text{for } k \in \mathbb{N}, \quad (26)$$

where  $\mathbf{a}^{(0)} \in \mathbb{R}^n$ ,  $\mathbf{T}: \mathbb{R}^n \rightarrow \mathbb{R}^n$  is a linear operator, and  $\mathbf{q}: \mathbb{R}^n \rightarrow \mathbb{R}^n$  satisfies  $\lim_{t \rightarrow 0} \sup_{\|\mathbf{a}\| \leq t} \|\mathbf{q}(\mathbf{a})\| / \|\mathbf{a}\| = 0$ . The author showed that if the operator  $\mathbf{T}$  satisfies  $\|\mathbf{T}^k\|_2 \leq c(\zeta)(\rho + \zeta)^k$ , for some  $\rho < 1$  and arbitrarily small  $\zeta > 0$ , then  $\{\mathbf{a}^{(k)}\}_{k=0}^\infty$  approaches zero with sufficiently small  $\|\mathbf{a}^{(0)}\|$ :

$$\|\mathbf{a}^{(k)}\| \leq C(\zeta)\|\mathbf{a}^{(0)}\|(\rho + \zeta)^k. \quad (27)$$

Applying this result to (24) with  $\mathbf{a}^{(k)} = \boldsymbol{\delta}^{(k)}$  and  $\mathbf{T} = \mathbf{H}$ , one can show that the error vector of Algorithm 1 converges to  $\mathbf{0}$  provided that  $\rho(\mathbf{H}) < 1$  and  $\|\boldsymbol{\delta}^{(0)}\|$  is sufficiently small. However, Polyak's result in (27) does not specify how small  $\|\mathbf{a}^{(0)}\|$  is as well as how large the factor  $C(\zeta)$  is. On the other hand, we employ a more elaborate approach to provide the region of linear convergence and the bound on the convergence speed in explicit expressions, as in (12) and (15), respectively.

**Step 2:** Our approach to study the convergence of the nonlinear different equation of form (24) is to leverage the eigen-decomposition  $\mathbf{H} = \mathbf{Q}\boldsymbol{\Lambda}\mathbf{Q}^{-1}$  and consider the transformed error vector as follows.

**Lemma 3.** Let  $\tilde{\boldsymbol{\delta}}^{(k)} = \mathbf{Q}^{-1}\boldsymbol{\delta}^{(k)}$  be the transformed error vector. If (12) holds and the spectral radius of  $\mathbf{H}$  is strictly less than 1, i.e.,  $\rho(\mathbf{H}) < 1$ , then, for all  $k \in \mathbb{N}$ , we have

$$\tilde{\boldsymbol{\delta}}^{(k+1)} = \boldsymbol{\Lambda}\tilde{\boldsymbol{\delta}}^{(k)} + \mathbf{q}_3(\tilde{\boldsymbol{\delta}}^{(k)}), \quad (28)$$

where the residual  $\mathbf{q}_3(\tilde{\boldsymbol{\delta}}^{(k)}) = \mathbf{Q}^{-1}\mathbf{q}_2(\mathbf{Q}\tilde{\boldsymbol{\delta}}^{(k)})$  satisfies  $\|\mathbf{q}_3(\tilde{\boldsymbol{\delta}}^{(k)})\| \leq (q/\|\mathbf{Q}^{-1}\|_2)\|\tilde{\boldsymbol{\delta}}^{(k)}\|^2$  for  $q$  given in (14).

The proof of Lemma 3 is given in Appendix E. Taking the norms of both sides of (28) and applying the triangle inequality, we obtain

$$\|\tilde{\boldsymbol{\delta}}^{(k+1)}\| \leq \rho(\mathbf{H})\|\tilde{\boldsymbol{\delta}}^{(k)}\| + \frac{q}{\|\mathbf{Q}^{-1}\|_2}\|\tilde{\boldsymbol{\delta}}^{(k)}\|^2. \quad (29)$$

This inequality, holding for all  $k \in \mathbb{N}$ , is the key to the convergence of the transformed error sequence in the next step.

**Step 3:** If we replace the inequality symbol in (29) by the equality symbol, then we obtain an asymptotically-linear quadratic difference equation whose convergence is studied in [49]. Indeed, the following lemma states that the norm of the transformed error vector is governed by this asymptotically-linear quadratic system dynamic:

**Lemma 4.** Assume the same setting as Lemma 3. Then, for any desired accuracy  $0 < \tilde{\epsilon} < 1$ , we have  $\|\tilde{\boldsymbol{\delta}}^{(k)}\| \leq \tilde{\epsilon}\|\tilde{\boldsymbol{\delta}}^{(0)}\|$  for all

$$k \geq \frac{\log(1/\tilde{\epsilon})}{\log(1/\rho(\mathbf{H}))} + c_3(\rho(\mathbf{H}), \tau), \quad (30)$$

where  $\tau = q\|\tilde{\boldsymbol{\delta}}^{(0)}\|/\|\mathbf{Q}^{-1}\|_2/(1 - \rho(\mathbf{H})) \in (0, 1)$  and

$$c_3(\rho, \tau) = \frac{1}{\rho \log(1/\rho)} \left( E_1\left(\log \frac{1}{\rho + \tau(1 - \rho)}\right) - E_1\left(\log \frac{1}{\rho}\right) + \frac{1}{2} \cdot \log\left(\frac{\log(1/\rho)}{\log(1/(\rho + \tau(1 - \rho)))}\right) \right) + 1, \quad (31)$$

for  $E_1(t) = \int_t^\infty \frac{e^{-z}}{z} dz$  being the exponential integral [51].

The proof of Lemma 4 is given in Appendix F.

**Step 4:** Finally, we show the convergence of  $\|\boldsymbol{\delta}^{(k)}\|$  based on the convergence of  $\|\tilde{\boldsymbol{\delta}}^{(k)}\|$ . From (30), substituting  $\tilde{\epsilon} = \epsilon/\kappa(\mathbf{Q})$  and identifying  $c_3$  as  $c_3(\rho(\mathbf{H}), \tau)$ , we obtain (15). Thus, it remains to prove that the accuracy on the transformed error vector  $\|\tilde{\boldsymbol{\delta}}^{(k)}\| \leq \tilde{\epsilon}\|\tilde{\boldsymbol{\delta}}^{(0)}\|$  is sufficient for the accuracy on the original error vector  $\|\boldsymbol{\delta}^{(k)}\| \leq \epsilon\|\boldsymbol{\delta}^{(0)}\|$ . Indeed, given

$$\|\boldsymbol{\delta}^{(k)}\| \leq \tilde{\epsilon}\|\tilde{\boldsymbol{\delta}}^{(0)}\| = \frac{\epsilon}{\|\mathbf{Q}\|_2\|\mathbf{Q}^{-1}\|_2}\|\tilde{\boldsymbol{\delta}}^{(0)}\|,$$

we have

$$\begin{aligned} \|\delta^{(k)}\| &= \|\mathbf{Q}\tilde{\delta}^{(k)}\| \leq \|\mathbf{Q}\|_2 \|\tilde{\delta}^{(k)}\| \\ &\leq \|\mathbf{Q}\|_2 \cdot \frac{\epsilon}{\|\mathbf{Q}\|_2 \|\mathbf{Q}^{-1}\|_2} \|\tilde{\delta}^{(0)}\| \\ &= \frac{\epsilon}{\|\mathbf{Q}^{-1}\|_2} \|\tilde{\delta}^{(0)}\| \leq \epsilon \|\delta^{(0)}\|, \end{aligned}$$

where the last inequality stems from  $\|\tilde{\delta}^{(0)}\| = \|\mathbf{Q}^{-1}\delta^{(0)}\| \leq \|\mathbf{Q}^{-1}\|_2 \|\delta^{(0)}\|$ . This completes our proof of Theorem 1.

## V. APPLICATIONS

In this section, we demonstrate the application of our proposed framework to a collection of machine learning and signal processing problems. For some problems, we show that the obtained asymptotic rate of convergence matches existing results in the literature. For other problems (e.g., matrix completion) in which the exact asymptotic convergence rate of PGD has not been studied, we verify the rate obtained by our analysis against the rate of convergence obtained in numerical experiments. While we have not seen similar results for such problems in the literature, our goal here is not to claim the originality of the result but to illustrate the general recipe for asymptotic convergence analysis. Table I describes the steps we follow to obtain the asymptotic linear rate and the region of linear convergence in each application. Table II summarizes our local convergence result on the four problems presented in this section. The detailed analysis is given below.

### A. Linearly Constrained Least Squares

As a sanity check, we start with a simple example of the so-called linearly constrained least squares (LCLS)

$$\min_{\mathbf{x} \in \mathbb{R}^n} \frac{1}{2} \|\mathbf{A}\mathbf{x} - \mathbf{b}\|^2 \quad \text{s.t. } \mathbf{C}\mathbf{x} = \mathbf{d}, \quad (32)$$

where  $\mathbf{A} \in \mathbb{R}^{m \times n}$ ,  $\mathbf{b} \in \mathbb{R}^m$ ,  $\mathbf{C} \in \mathbb{R}^{p \times n}$ , and  $\mathbf{d} \in \mathbb{R}^p$ . In addition, we assume that  $p < n$  and  $\mathbf{C}$  has linearly independent rows. While this problem can be solved efficiently using the method of Lagrange multipliers [52] or the method of weighting [53], we limit our interest to using PGD to solve (32) to demonstrate the applicability of our analysis.<sup>2</sup>

**Step 1:** In this example,  $\mathbf{A}$  and  $\mathbf{b}$  are given explicitly in (32). The constraint set  $\mathcal{C}$  is the closed convex affine subspace

$$\mathbb{T} = \{\mathbf{x} \in \mathbb{R}^n \mid \mathbf{C}\mathbf{x} = \mathbf{d}\}.$$

The orthogonal projection onto this subspace is given in a closed-form expression as  $\mathcal{P}_{\mathcal{C}}(\mathbf{x}) = \mathbf{x} - \mathbf{C}^{\top}(\mathbf{C}\mathbf{C}^{\top})^{-1}(\mathbf{C}\mathbf{x} - \mathbf{d})$ , for all  $\mathbf{x} \in \mathbb{R}^n$  [58]. Since  $\mathbf{C}$  has full row rank, it admits a compact singular value decomposition (SVD)  $\mathbf{C} = \mathbf{U}_C \Sigma_C \mathbf{V}_C^{\top}$ , where  $\Sigma_C \in \mathbb{R}^{p \times p}$  is a diagonal matrix with positive diagonal entries,  $\mathbf{U}_C \in \mathbb{R}^{p \times p}$  and  $\mathbf{V}_C \in \mathbb{R}^{n \times p}$  satisfy  $\mathbf{U}_C^{\top} \mathbf{U}_C = \mathbf{V}_C^{\top} \mathbf{V}_C = \mathbf{I}_p$ . Denote  $\mathbf{V}_C^{\perp} \in \mathbb{R}^{n \times (n-p)}$  the orthogonal complement of  $\mathbf{V}_C$ , i.e.,  $\mathbf{V}_C^{\perp} (\mathbf{V}_C^{\perp})^{\top} = \mathbf{I}_n - \mathbf{V}_C \mathbf{V}_C^{\top}$  and  $(\mathbf{V}_C^{\perp})^{\top} \mathbf{V}_C^{\perp} = \mathbf{I}_{n-p}$ . Substituting the SVD of  $\mathbf{C}$  back into the aforementioned expression of  $\mathcal{P}_{\mathcal{C}}$  yields

$$\mathcal{P}_{\mathcal{C}}(\mathbf{x}) = \mathbf{V}_C^{\perp} (\mathbf{V}_C^{\perp})^{\top} \mathbf{x} + \tilde{\mathbf{d}}, \quad (33)$$

<sup>2</sup>In the literature, this algorithm is referred to as the projected Landweber iteration [54]–[57].

<b>Step 1:</b>	Identify $\mathbf{A}$ , $\mathbf{b}$ , $\mathcal{C}$ , and $\mathcal{P}_{\mathcal{C}}$ .
<b>Step 2:</b>	Establish the conditions for $\mathbf{x}^* \in \mathcal{C}$ to be a <b>Lipschitz stationary point</b> of (1). In particular, (i) $\mathcal{P}_{\mathcal{C}}$ is Lipschitz-continuously differentiable at every $\mathbf{x}^*$ with $\nabla \mathcal{P}_{\mathcal{C}}(\mathbf{x}^*)$ , $c_1(\mathbf{x}^*)$ , and $c_2(\mathbf{x}^*)$ ; and (ii) the stationarity equation (7) holds.
<b>Step 3:</b>	Establish the conditions for $\eta > 0$ such that (i) $\mathbf{x}^*$ is a <b>fixed point</b> of Algorithm 1 with step size $\eta$ , i.e., $\mathbf{x}^* = \mathcal{P}_{\mathcal{C}}(\mathbf{z}_{\eta}^*)$ , for $\mathbf{z}_{\eta}^* = \mathbf{x}^* - \eta \mathbf{A}^{\top}(\mathbf{A}\mathbf{x}^* - \mathbf{b})$ ; and (ii) $\mathcal{P}_{\mathcal{C}}$ is Lipschitz-continuously differentiable at $\mathbf{z}_{\eta}^*$ with $\nabla \mathcal{P}_{\mathcal{C}}(\mathbf{z}_{\eta}^*)$ , $c_1(\mathbf{z}_{\eta}^*)$ , and $c_2(\mathbf{z}_{\eta}^*)$ .
<b>Step 4:</b>	Determine the <b>asymptotic linear rate</b> $\rho$ as the spectral radius of $\mathbf{H}$ given by (11). (If $\nabla \mathcal{P}_{\mathcal{C}}(\mathbf{z}_{\eta}^*) = \nabla \mathcal{P}_{\mathcal{C}}(\mathbf{x}^*)$ , (18) can be used instead.)
<b>Step 5:</b>	Establish the conditions for $\rho < 1$ , which guarantees local linear convergence. Thereby, combine these conditions with the previous conditions obtained from Steps 2 and 3.
<b>Step 6:</b>	If $\mathbf{H}$ is diagonalizable, determine the <b>region of linear convergence</b> given by (12). (If $\nabla \mathcal{P}_{\mathcal{C}}(\mathbf{z}_{\eta}^*) = \nabla \mathcal{P}_{\mathcal{C}}(\mathbf{x}^*)$ , (19) can be used instead.)

TABLE I: General recipe for local convergence analysis.

where  $\tilde{\mathbf{d}} = \mathbf{V}_C \Sigma_C^{-1} \mathbf{U}_C^{\top} \mathbf{d} = \mathbf{C}^{\dagger} \mathbf{d}$ .

**Step 2:** From (33), we obtain the difference between the two projections of  $\mathbf{x} + \delta$  and  $\mathbf{x}$  onto  $\mathcal{C}$ , for any  $\mathbf{x}, \delta \in \mathbb{R}^n$ , as  $\mathcal{P}_{\mathcal{C}}(\mathbf{x} + \delta) - \mathcal{P}_{\mathcal{C}}(\mathbf{x}) = \mathbf{V}_C^{\perp} (\mathbf{V}_C^{\perp})^{\top} \delta$ . Using Definition 1 with the note that  $\Pi_{\mathcal{C}}(\mathbf{x} + \delta)$  is always singleton, we have  $\mathcal{P}_{\mathcal{C}}$  is Lipschitz-continuously differentiable at every  $\mathbf{x} \in \mathbb{R}^n$  with

$$\nabla \mathcal{P}_{\mathcal{C}}(\mathbf{x}) = \mathbf{V}_C^{\perp} (\mathbf{V}_C^{\perp})^{\top}, \quad c_1(\mathbf{x}) = \infty, \quad c_2(\mathbf{x}) = 0. \quad (34)$$

Due to the independence from  $\mathbf{x}$ , we also have  $\mathcal{P}_{\mathcal{C}}$  is Lipschitz-continuously differentiable at every  $\mathbf{x}^* \in \mathcal{C}$  with

$$\nabla \mathcal{P}_{\mathcal{C}}(\mathbf{x}^*) = \mathbf{V}_C^{\perp} (\mathbf{V}_C^{\perp})^{\top}, \quad c_1(\mathbf{x}^*) = \infty, \quad c_2(\mathbf{x}^*) = 0.$$

Next, substituting  $\nabla \mathcal{P}_{\mathcal{C}}(\mathbf{x}^*) = \mathbf{V}_C^{\perp} (\mathbf{V}_C^{\perp})^{\top}$  into the stationarity equation (7) yields  $\mathbf{V}_C^{\perp} (\mathbf{V}_C^{\perp})^{\top} \mathbf{A}^{\top} (\mathbf{A}\mathbf{x}^* - \mathbf{b}) = \mathbf{0}$ . Since  $\mathbf{V}_C^{\perp} \in \mathbb{R}^{n \times (n-p)}$  has full-rank, we can omit the left most  $\mathbf{V}_C^{\perp}$  and obtain the condition for  $\mathbf{x}^* \in \mathcal{C}$  to be a Lipschitz stationary point of (32) as

$$(\mathbf{A}\mathbf{V}_C^{\perp})^{\top} (\mathbf{A}\mathbf{x}^* - \mathbf{b}) = \mathbf{0}, \quad (35)$$

which means  $\mathbf{A}\mathbf{x}^* - \mathbf{b}$  is in the left null space of  $\mathbf{A}\mathbf{V}_C^{\perp}$ .<sup>3</sup>

**Step 3:** Evaluating the projection in (33) at  $\mathbf{z}_{\eta}^* = \mathbf{x}^* - \eta \mathbf{A}^{\top}(\mathbf{A}\mathbf{x}^* - \mathbf{b})$  and using the stationarity condition (35) to eliminate the term  $\eta \mathbf{V}_C^{\perp} (\mathbf{V}_C^{\perp})^{\top} \mathbf{A}^{\top} (\mathbf{A}\mathbf{x}^* - \mathbf{b})$ , we have  $\mathcal{P}_{\mathcal{C}}(\mathbf{z}_{\eta}^*) = \mathbf{x}^*$  for any  $\eta > 0$ . Thus, the condition in this step for  $\mathbf{x}^*$  to be a fixed point of Algorithm 1 is  $\eta > 0$ . In addition, substituting  $\mathbf{x} = \mathbf{z}_{\eta}^*$  into (34), we obtain  $\mathcal{P}_{\mathcal{C}}$  is Lipschitz-continuously differentiable at  $\mathbf{z}_{\eta}^*$  with

$$\nabla \mathcal{P}_{\mathcal{C}}(\mathbf{z}_{\eta}^*) = \mathbf{V}_C^{\perp} (\mathbf{V}_C^{\perp})^{\top}, \quad c_1(\mathbf{z}_{\eta}^*) = \infty, \quad c_2(\mathbf{z}_{\eta}^*) = 0.$$

**Step 4:** Since  $\nabla \mathcal{P}_{\mathcal{C}}(\mathbf{z}_{\eta}^*) = \nabla \mathcal{P}_{\mathcal{C}}(\mathbf{x}^*) = \mathbf{V}_C^{\perp} (\mathbf{V}_C^{\perp})^{\top}$ , using (18), we obtain the asymptotic linear rate as

$$\rho = \max\{|1 - \eta \lambda_1|, |1 - \eta \lambda_{n-p}|\}, \quad (36)$$

where  $\lambda_1$  and  $\lambda_{n-p}$  are the largest and smallest eigenvalues of  $(\mathbf{A}\mathbf{V}_C^{\perp})^{\top} \mathbf{A}\mathbf{V}_C^{\perp}$ , respectively.

<sup>3</sup>Here, it is interesting to note that any stationary point of (32) is a global minimizer since (32) is a convex optimization problem.

Problem formulation	Condition(s) for linear convergence	Asymptotic rate of convergence $\rho$	Region of convergence
$\min \frac{1}{2} \ \mathbf{A}\mathbf{x} - \mathbf{b}\ ^2$ s.t. $\mathbf{C}\mathbf{x} = \mathbf{d}$	$\left\{ \begin{array}{l} \mathbf{K} = (\mathbf{A}\mathbf{V}_C^\perp)^\top \mathbf{A}\mathbf{V}_C^\perp \text{ has full rank} \\ 0 < \eta < 2/\ \mathbf{A}\mathbf{V}_C^\perp\ _2^2 \end{array} \right.$	$\max\{ 1 - \eta\lambda_1(\mathbf{K}) ,  1 - \eta\lambda_{n-p}(\mathbf{K}) \}$	$\ \mathbf{x} - \mathbf{x}^*\  < \infty$
$\min \frac{1}{2} \ \mathbf{A}\mathbf{x} - \mathbf{b}\ ^2$ s.t. $\ \mathbf{x}\ _0 \leq s$	$\left\{ \begin{array}{l} \mathbf{K} = (\mathbf{A}\mathbf{S}_{\mathbf{x}^*})^\top \mathbf{A}\mathbf{S}_{\mathbf{x}^*} \text{ has full rank} \\ 0 < \eta < \min\left\{\frac{2}{\ \mathbf{A}\mathbf{S}_{\mathbf{x}^*}\ _2^2}, \frac{ x_{[s]}^* }{\ \mathbf{v}^*\ _\infty}\right\} \end{array} \right.$	$\max\{ 1 - \eta\lambda_1(\mathbf{K}) ,  1 - \eta\lambda_s(\mathbf{K}) \}$	$\ \mathbf{x} - \mathbf{x}^*\  < \min\left\{\frac{ x_{[s]}^* }{\sqrt{2}}, \frac{ x_{[s]}^*  - \eta\ \mathbf{v}^*\ _\infty}{\sqrt{2}\ \mathbf{I}_n - \eta\mathbf{A}^\top\mathbf{A}\ _2}\right\}$
$\min \frac{1}{2} \ \mathbf{A}\mathbf{x} - \mathbf{b}\ ^2$ s.t. $\ \mathbf{x}\  = 1$	$\left\{ \begin{array}{l} 0 < \eta < \infty \quad \text{if } \gamma \leq -\lambda_1(\mathbf{K}) \\ 0 < \eta < \frac{2}{\gamma + \lambda_1(\mathbf{K})} \quad \text{o.t.w.} \end{array} \right.$	$\frac{1}{1-\eta\gamma} \max\{ 1 - \eta\lambda_1(\mathbf{K}) ,  1 - \eta\lambda_{n-1}(\mathbf{K}) \}$	$\ \mathbf{x} - \mathbf{x}^*\  \leq \frac{1-\rho}{2(t^2+t)}, t = \frac{\ \mathbf{I}_n - \eta\mathbf{A}^\top\mathbf{A}\ _2}{1-\eta\gamma}$
$\min \frac{1}{2} \ \mathcal{P}_\Omega(\mathbf{X} - \mathbf{M})\ _F^2$ s.t. $\text{rank}(\mathbf{X}) \leq r$	$\left\{ \begin{array}{l} \mathbf{K} = \mathbf{Q}_\perp^\top \mathbf{S}_\Omega \mathbf{S}_\Omega^\top \mathbf{Q}_\perp \text{ has full rank} \\ 0 < \eta < \frac{2}{\ \mathbf{Q}_\perp^\top \mathbf{S}_\Omega \mathbf{S}_\Omega^\top \mathbf{Q}_\perp\ _2} \end{array} \right.$	$\max\{ 1 - \eta\lambda_1(\mathbf{K}) ,  1 - \eta\lambda_{r(m+n-r)}(\mathbf{K}) \}$	$\ \mathbf{X} - \mathbf{X}^*\ _F \leq \frac{1-\rho}{8(1+\sqrt{2})}$

TABLE II: Summary of local convergence analysis for four problems: linearly constrained least squares (Sec. V-A), sparse recovery (Sec. V-B), least squares with a unit norm constraint (Sec. V-C), and matrix completion (Sec. V-D). In the second row,  $\mathbf{v}^* = \mathbf{A}^\top(\mathbf{A}\mathbf{x}^* - \mathbf{b})$ . In the third row,  $\mathbf{K} = (\mathbf{A}\mathbf{U}_{\mathbf{x}^*})^\top \mathbf{A}\mathbf{U}_{\mathbf{x}^*}$ . We refer the reader to each of the corresponding sections for further details.

**Step 5:** From (36), we have  $\rho < 1$  if and only if  $(\mathbf{A}\mathbf{V}_C^\perp)^\top \mathbf{A}\mathbf{V}_C^\perp$  has full rank and  $0 < \eta < 2/\|\mathbf{A}\mathbf{V}_C^\perp\|_2^2$ . It is noted that the latter condition is sufficient for the condition  $\eta > 0$  in Step 3.

**Step 6:** Since  $c_1(\mathbf{x}^*) = c_1(\mathbf{z}_\eta^*) = \infty$  and  $c_2(\mathbf{x}^*) = c_2(\mathbf{z}_\eta^*) = 0$ , the region of convergence given by (19) is the entire space  $\mathbb{R}^n$ , which implies global convergence.

**Remark 4.** The explicit expression of the convergence rate in (36) offers a simple method to select the optimal step size:

$$\begin{aligned} \eta_{opt} &= \underset{0 < \eta < 2/\|\mathbf{A}\mathbf{V}_C^\perp\|_2^2}{\operatorname{argmin}} \max\{|1 - \eta\lambda_1|, |1 - \eta\lambda_{n-p}|\} \\ &= \frac{2}{\lambda_1 + \lambda_{n-p}}. \end{aligned} \quad (37)$$

Using  $\eta = \eta_{opt}$ , we obtain the optimal rate of convergence

$$\rho_{opt} = 1 - \frac{2}{\kappa((\mathbf{A}\mathbf{V}_C^\perp)^\top \mathbf{A}\mathbf{V}_C^\perp) + 1}. \quad (38)$$

As a comparison, the optimal convergence rate of gradient descent for the unconstrained problem is given by [47]

$$u_{opt} = 1 - \frac{2}{\kappa(\mathbf{A}^\top\mathbf{A}) + 1}.$$

Recall from Remark 2 that  $\rho_{opt} \leq u_{opt}$  due to the interlacing of eigenvalues of  $(\mathbf{A}\mathbf{V}_C^\perp)^\top \mathbf{A}\mathbf{V}_C^\perp$  and  $\mathbf{A}^\top\mathbf{A}$ .

### B. Iterative Hard Thresholding for Sparse Recovery

In compressed sensing, one would like to reconstruct a sparse signal by finding solutions to under-determined linear systems  $\mathbf{A}\mathbf{x} = \mathbf{b}$ , where  $\mathbf{A} \in \mathbb{R}^{m \times n}$  and  $\mathbf{b} \in \mathbb{R}^m$  (for  $m < n$ ). This problem can be formulated as an L0-norm constrained least squares:

$$\min_{\mathbf{x} \in \mathbb{R}^n} \frac{1}{2} \|\mathbf{A}\mathbf{x} - \mathbf{b}\|^2 \quad \text{s.t. } \|\mathbf{x}\|_0 \leq s. \quad (39)$$

In the literature, the PGD algorithm for solving (39) is often known as iterative hard thresholding (IHT). The convergence of a special case of IHT in which  $\|\mathbf{A}\|_2 < 1$  and  $\eta = 1$  has been well-studied in [2], [3], under the restricted isometry property (RIP) assumption on  $\mathbf{A}$ . In the following, we

demonstrate the application of our framework to establishing a local convergence analysis of IHT with a range of different step sizes, without requiring the RIP of  $\mathbf{A}$ .

**Step 1:** In this example,  $\mathbf{A}$  and  $\mathbf{b}$  are given explicitly in (39), and the constraint set  $\mathcal{C}$  is the closed non-convex set of  $s$ -sparse vectors

$$\Phi_{\leq s} = \{\mathbf{x} \in \mathbb{R}^n \mid \|\mathbf{x}\|_0 \leq s\},$$

with the projection  $\mathcal{P}_C : \mathbb{R}^n \rightarrow \mathbb{R}^n$  given by [2]

$$[\mathcal{P}_C(\mathbf{x})]_i = \begin{cases} 0 & \text{if } |x_i| < |x_{[s]}| \\ x_i & \text{if } |x_i| \geq |x_{[s]}| \end{cases} \quad \text{for } i = 1, \dots, n, \quad (40)$$

where  $x_i$  and  $x_{[s]}$  denote the  $i$ th coordinate and the  $s$ th-largest (in magnitude) element of a vector  $\mathbf{x} \in \mathbb{R}^n$ , respectively. In the case  $\mathbf{x}$  has multiple elements with the same magnitude as  $x_{[s]}$ , e.g.,  $x_{[s]} = x_{[s+1]} > 0$ , we sort these entries based on the (descending) lexicographical order so that (40) is well-defined.

**Step 2:** In contrast to the previous example, the projection here is non-linear and non-unique since the set  $\Phi_{\leq s}$  is a real algebraic variety but not smooth in those points in  $\mathbb{R}^n$  of sparsity strictly less than  $s$ . The smooth part of  $\Phi_{\leq s}$ , notwithstanding, is the subset

$$\Phi_{=s} = \{\mathbf{x} \in \mathbb{R}^n \mid \|\mathbf{x}\|_0 = s\}$$

of vectors with exactly  $s$  non-zero elements. In Appendix G, we show that any  $\mathbf{x}^* \in \Phi_{=s}$  and  $\mathbf{x} \in \mathcal{B}(\mathbf{x}^*, |x_{[s]}^*|/\sqrt{2})$  share the same index set of  $s$ -largest elements (in magnitude), denoted by  $\Omega_s(\mathbf{x}^*)$ .<sup>4</sup> Let the indices in  $\Omega_s(\mathbf{x}^*)$  be  $i_1 \leq \dots \leq i_s$  and  $\mathbf{S}_{\mathbf{x}^*} = [e_{i_1}, \dots, e_{i_s}] \in \mathbb{R}^{n \times s}$ . Then, we have  $(\mathbf{S}_{\mathbf{x}^*})^\top \mathbf{S}_{\mathbf{x}^*} = \mathbf{I}_s$  and

$$\mathcal{P}_C(\mathbf{x}) = \mathbf{S}_{\mathbf{x}^*} \mathbf{S}_{\mathbf{x}^*}^\top \mathbf{x}, \quad \forall \mathbf{x} \in \mathcal{B}(\mathbf{x}^*, |x_{[s]}^*|/\sqrt{2}). \quad (41)$$

By Definition 1, we obtain  $\mathcal{P}_C$  is Lipschitz-continuously differentiable at any  $\mathbf{x}^* \in \Phi_{=s}$  with

$$\nabla \mathcal{P}_C(\mathbf{x}^*) = \mathbf{S}_{\mathbf{x}^*} \mathbf{S}_{\mathbf{x}^*}^\top, \quad c_1(\mathbf{x}^*) = \frac{1}{\sqrt{2}} |x_{[s]}^*|, \quad c_2(\mathbf{x}^*) = 0.$$

<sup>4</sup>It is interesting to note that  $|x_{[s]}^*|/\sqrt{2}$  is the largest possible radius. A counter-example is also constructed in Appendix G.

Similar to the previous example, the stationarity equation for  $\mathbf{x}^* \in \Phi_{=s}$  is given by

$$(\mathbf{A}\mathbf{S}_{\mathbf{x}^*})^\top(\mathbf{A}\mathbf{x}^* - \mathbf{b}) = \mathbf{0}. \quad (42)$$

Thus, we obtain the conditions for  $\mathbf{x}^* \in \mathcal{C}$  to be a Lipschitz stationary point of (39) are  $\mathbf{x}^* \in \Phi_{=s}$  and the vector  $\mathbf{v}^* = \mathbf{A}^\top(\mathbf{A}\mathbf{x}^* - \mathbf{b})$  satisfies  $v_i^* = 0$  for all  $i \in \Omega_s(\mathbf{x}^*)$ .

**Step 3:** First, we show that the condition in this step for  $\mathbf{x}^*$  to be a fixed point of Algorithm 1 is

$$0 < \eta < \frac{|x_{[s]}^*|}{\|\mathbf{v}^*\|_\infty}. \quad (43)$$

Since  $v_i^* = 0$  for all  $i \in \Omega_s(\mathbf{x}^*)$ , we have  $\mathbf{z}_\eta^* = \mathbf{x}^* - \eta\mathbf{v}^*$  satisfies  $(z_\eta^*)_i = x_i^*$  for all  $i \in \Omega_s(\mathbf{x}^*)$ . Moreover, for any indices  $i \in \Omega_s(\mathbf{x}^*)$  and  $j \in \{1, \dots, n\} \setminus \Omega_s(\mathbf{x}^*)$ , we have

$$\begin{aligned} |(z_\eta^*)_j| &= |x_j^* - \eta v_j^*| = \eta |v_j^*| \\ &< \frac{|x_{[s]}^*|}{\|\mathbf{v}^*\|_\infty} |v_j^*| \leq |x_{[s]}^*| \leq |x_i^*| = |(z_\eta^*)_i|, \end{aligned}$$

where the second inequality stems from  $|v_j^*| \leq \|\mathbf{v}^*\|_\infty$ . Therefore,  $\Omega_s(\mathbf{x}^*)$  contains the  $s$ -largest (in magnitude) elements of  $\mathbf{z}_\eta^*$ , and hence,  $\mathbf{x}^* = \mathcal{P}_\mathcal{C}(\mathbf{z}_\eta^*)$ .

Second, we consider the Lipschitz-continuous differentiability of  $\mathcal{P}_\mathcal{C}$  at  $\mathbf{z}_\eta^*$ . Given  $\eta$  in (43), by the same argument as in Appendix G, one can show that every point in  $\mathcal{B}(\mathbf{z}_\eta^*, (|(z_\eta^*)_{[s]}| - |(z_\eta^*)_{[s+1]}|)/\sqrt{2})$  shares the same index set of  $s$ -largest elements (in magnitude) with  $\mathbf{z}_\eta^*$ , which is essentially  $\Omega_s(\mathbf{x}^*)$ . Here, we note that  $|(z_\eta^*)_{[s]}| - |(z_\eta^*)_{[s+1]}| = |x_{[s]}^*| - \eta\|\mathbf{v}^*\|_\infty$ . Thus, we obtain  $\mathcal{P}_\mathcal{C}$  is Lipschitz-continuously differentiable at  $\mathbf{z}_\eta^*$  with

$$\begin{aligned} \nabla \mathcal{P}_\mathcal{C}(\mathbf{z}_\eta^*) &= \mathbf{S}_{\mathbf{x}^*} \mathbf{S}_{\mathbf{x}^*}^\top, \quad c_2(\mathbf{z}_\eta^*) = 0, \\ c_1(\mathbf{z}_\eta^*) &= \frac{1}{\sqrt{2}} (|x_{[s]}^*| - \eta\|\mathbf{v}^*\|_\infty). \end{aligned}$$

**Step 4:** Since  $\nabla \mathcal{P}_\mathcal{C}(\mathbf{z}_\eta^*) = \nabla \mathcal{P}_\mathcal{C}(\mathbf{x}^*) = \mathbf{S}_{\mathbf{x}^*} \mathbf{S}_{\mathbf{x}^*}^\top$ , using (18), we obtain the asymptotic linear rate as

$$\rho = \max\{|1 - \eta\lambda_1|, |1 - \eta\lambda_s|\}. \quad (44)$$

where  $\lambda_1$  and  $\lambda_s$  are the largest and smallest eigenvalues of  $(\mathbf{A}\mathbf{S}_{\mathbf{x}^*})^\top \mathbf{A}\mathbf{S}_{\mathbf{x}^*}$ , respectively.

**Step 5:** From (44),  $\rho < 1$  if and only if  $(\mathbf{A}\mathbf{S}_{\mathbf{x}^*})^\top \mathbf{A}\mathbf{S}_{\mathbf{x}^*}$  has full rank and

$$0 < \eta < \frac{2}{\|\mathbf{A}\mathbf{S}_{\mathbf{x}^*}\|_2^2}. \quad (45)$$

Combining (43) and (45) yields the condition on the step size

$$0 < \eta < \min\left\{\frac{2}{\|\mathbf{A}\mathbf{S}_{\mathbf{x}^*}\|_2^2}, \frac{|x_{[s]}^*|}{\|\mathbf{A}^\top(\mathbf{A}\mathbf{x}^* - \mathbf{b})\|_\infty}\right\}.$$

**Step 6:** Recall that  $c_2(\mathbf{x}^*) = c_2(\mathbf{z}_\eta^*) = 0$ . From (19), the region of convergence is given by

$$\|\mathbf{x} - \mathbf{x}^*\| < \min\left\{\frac{|x_{[s]}^*|}{\sqrt{2}}, \frac{|x_{[s]}^*| - \eta\|\mathbf{v}^*\|_\infty}{\sqrt{2}\|\mathbf{I}_n - \eta\mathbf{A}^\top\mathbf{A}\|_2}\right\}.$$

**Remark 5.** In Appendix G, we further show that any stationary point  $\mathbf{x}^*$  of (39) must be a local minimum of (39). Moreover, the condition  $(\mathbf{A}\mathbf{S}_{\mathbf{x}^*})^\top \mathbf{A}\mathbf{S}_{\mathbf{x}^*}$  has full rank in Step 5

implies  $\mathbf{x}^*$  is a strict local minimum of (39). Finally, it is interesting to note that for  $\eta = 1/\|\mathbf{A}\|_2^2$ , we recover the same rate of linear convergence given in [2].

### C. Least Squares with the Unit Norm Constraint

A common constraint that arises in regularization methods for ill-posed problems is the spherical constraint [9], [59], [60]. In particular, we consider the following optimization problem

$$\min_{\mathbf{x} \in \mathbb{R}^n} \frac{1}{2} \|\mathbf{A}\mathbf{x} - \mathbf{b}\|^2 \quad \text{s.t. } \|\mathbf{x}\| = 1, \quad (46)$$

where  $\mathbf{A} \in \mathbb{R}^{m \times n}$  and  $\mathbf{b} \in \mathbb{R}^m$ .

**Step 1:** In this example,  $\mathbf{A}$  and  $\mathbf{b}$  are given explicitly in (46), and the constraint set  $\mathcal{C}$  is the closed non-convex sphere

$$\mathcal{S} = \{\mathbf{x} \in \mathbb{R}^n \mid \|\mathbf{x}\| = 1\},$$

with the projection  $\mathcal{P}_\mathcal{C} : \mathbb{R}^n \rightarrow \mathbb{R}^n$  given by

$$\mathcal{P}_\mathcal{C}(\mathbf{x}) = \begin{cases} \frac{\mathbf{x}}{\|\mathbf{x}\|} & \text{if } \mathbf{x} \neq \mathbf{0}, \\ \mathbf{e}_1 & \text{if } \mathbf{x} = \mathbf{0}. \end{cases} \quad (47)$$

**Step 2:** In Example 1, we showed that the projection onto the unit sphere is Lipschitz-continuously differentiable at any  $\mathbf{x} \neq \mathbf{0}$ . Since  $\mathbf{0} \notin \mathcal{C}$ , we have  $\mathcal{P}_\mathcal{C}$  is Lipschitz-continuously differentiable at every  $\mathbf{x}^* \in \mathcal{C}$  with

$$\nabla \mathcal{P}_\mathcal{C}(\mathbf{x}^*) = \mathbf{I}_n - \mathbf{x}^*(\mathbf{x}^*)^\top, \quad c_1(\mathbf{x}^*) = \infty, \quad c_2(\mathbf{x}^*) = 2.$$

In addition, substituting  $\nabla \mathcal{P}_\mathcal{C}(\mathbf{x}^*) = \mathbf{I}_n - \mathbf{x}^*(\mathbf{x}^*)^\top$  into the stationarity equation (7) yields  $(\mathbf{I}_n - \mathbf{x}^*(\mathbf{x}^*)^\top)\mathbf{A}^\top(\mathbf{A}\mathbf{x}^* - \mathbf{b}) = \mathbf{0}$ . Equivalently, we have

$$\mathbf{A}^\top(\mathbf{A}\mathbf{x}^* - \mathbf{b}) = \gamma \mathbf{x}^*, \quad (48)$$

where  $\gamma = (\mathbf{x}^*)^\top \mathbf{A}^\top(\mathbf{A}\mathbf{x}^* - \mathbf{b})$  is the Lagrange multiplier at  $\mathbf{x}^*$  (see Lemma 1 in [35]). Thus, we obtain the condition for  $\mathbf{x}^* \in \mathcal{C}$  to be a Lipschitz stationary point of (46) is  $\mathbf{x}^*$  and  $\mathbf{A}^\top(\mathbf{A}\mathbf{x}^* - \mathbf{b})$  are collinear.

**Step 3:** First, the necessary condition for  $\mathcal{P}_\mathcal{C}$  to be Lipschitz-continuously differentiable at  $\mathbf{z}_\eta^*$  is  $\mathbf{z}_\eta^* \in \text{dom } \mathcal{P}_\mathcal{C}$ , i.e.,  $\mathbf{z}_\eta^* \neq \mathbf{0}$ . From (48), we have  $\mathbf{z}_\eta^* = \mathbf{x}^* - \eta\mathbf{A}^\top(\mathbf{A}\mathbf{x}^* - \mathbf{b}) = (1 - \eta\gamma)\mathbf{x}^*$ . Hence,  $\mathbf{z}_\eta^* \neq \mathbf{0}$  is equivalent to  $1 - \eta\gamma \neq 0$ . Now the projection  $\mathcal{P}_\mathcal{C}$  at  $\mathbf{z}_\eta^* \neq \mathbf{0}$  is given by

$$\mathcal{P}_\mathcal{C}(\mathbf{z}_\eta^*) = \frac{(1 - \eta\gamma)\mathbf{x}^*}{\|(1 - \eta\gamma)\mathbf{x}^*\|} = \frac{1 - \eta\gamma}{|1 - \eta\gamma|} \mathbf{x}^*,$$

which implies  $\mathbf{x}^* = \mathcal{P}_\mathcal{C}(\mathbf{z}_\eta^*)$  if and only if  $1 - \eta\gamma > 0$ . Thus, we obtain the condition for  $\eta > 0$  such that  $\mathbf{x}^*$  is a fixed point of Algorithm 1 and  $\mathcal{P}_\mathcal{C}$  is Lipschitz-continuously differentiable at  $\mathbf{z}_\eta^*$  is  $1 - \eta\gamma > 0$ , which is equivalent to

$$\begin{cases} \eta \in (0, \infty) & \text{if } \gamma \leq 0, \\ \eta \in (0, \frac{1}{\gamma}) & \text{if } \gamma > 0. \end{cases} \quad (49)$$

Second, it follows from (5) that  $\mathcal{P}_\mathcal{C}$  is Lipschitz-continuously differentiable at  $\mathbf{z}_\eta^*$  with

$$\begin{aligned} \nabla \mathcal{P}_\mathcal{C}(\mathbf{z}_\eta^*) &= \frac{1}{\|\mathbf{z}_\eta^*\|} \left( \mathbf{I}_n - \frac{\mathbf{z}_\eta^*(\mathbf{z}_\eta^*)^\top}{\|\mathbf{z}_\eta^*\|^2} \right) = \frac{\mathbf{I}_n - \mathbf{x}^*(\mathbf{x}^*)^\top}{1 - \eta\gamma}, \\ c_1(\mathbf{z}_\eta^*) &= \infty, \quad c_2(\mathbf{z}_\eta^*) = \frac{2}{\|\mathbf{z}_\eta^*\|^2} = \frac{2}{(1 - \eta\gamma)^2}. \end{aligned}$$

**Step 4:** Denote  $\mathbf{P}_{\mathbf{x}^*}^\perp = \mathbf{I}_n - \mathbf{x}^*(\mathbf{x}^*)^\top$ . From (11), the asymptotic linear rate is given by

$$\begin{aligned} \rho &= \rho \left( \frac{1}{1 - \eta\gamma} \mathbf{P}_{\mathbf{x}^*}^\perp (\mathbf{I}_n - \eta \mathbf{A}^\top \mathbf{A}) \mathbf{P}_{\mathbf{x}^*}^\perp \right) \\ &= \frac{1}{1 - \eta\gamma} \|\mathbf{P}_{\mathbf{x}^*}^\perp (\mathbf{I}_n - \eta \mathbf{A}^\top \mathbf{A}) \mathbf{P}_{\mathbf{x}^*}^\perp\|_2. \end{aligned}$$

Let  $\mathbf{P}_{\mathbf{x}^*}^\perp = \mathbf{U}_{\mathbf{x}^*} \mathbf{U}_{\mathbf{x}^*}^\top$ , where  $\mathbf{U}_{\mathbf{x}^*} \in \mathbb{R}^{n \times (n-1)}$  is a semi-orthogonal matrix whose columns provide a basis for the null space of  $\mathbf{x}^*$ . Then, following the same derivation as in the proof of Corollary 1, we obtain

$$\rho = \frac{1}{1 - \eta\gamma} \max\{|1 - \eta\lambda_1|, |1 - \eta\lambda_{n-1}|\}, \quad (50)$$

where  $\lambda_1$  and  $\lambda_{n-1}$  are the largest and smallest eigenvalues of  $(\mathbf{A}\mathbf{U}_{\mathbf{x}^*})^\top \mathbf{A}\mathbf{U}_{\mathbf{x}^*}$ , respectively.

**Step 5:** Since  $|1 - \eta\lambda| / (1 - \eta\gamma) < 1$  is equivalent to  $\eta\gamma - 1 < 1 - \eta\lambda < 1 - \eta\gamma$ , we have  $\rho < 1$  if and only if

$$\gamma < \lambda_{n-1} \quad (51)$$

and

$$\eta(\gamma + \lambda_1) < 2. \quad (52)$$

Similar to (49), the inequality in (52) can be rewritten as

$$\begin{cases} \eta \in (0, \infty) & \text{if } \gamma \leq -\lambda_1, \\ \eta \in (0, \frac{2}{\gamma + \lambda_1}) & \text{if } \gamma > -\lambda_1. \end{cases}$$

Finally, we note that conditions (51) and (52) together imply the condition  $1 - \eta\gamma > 0$  in Step 3 since  $2\eta\gamma < \eta(\gamma + \lambda_{n-1}) \leq \eta(\gamma + \lambda_1) < 2$ .

**Step 6:** To determine the region of linear convergence, we first recall that  $c_1(\mathbf{x}^*) = c_1(\mathbf{z}_\eta^*) = \infty$ . Second, we have

$$\|\nabla \mathcal{P}_c(\mathbf{z}_\eta^*)\|_2 = \left\| \frac{\mathbf{I}_n - \mathbf{x}^*(\mathbf{x}^*)^\top}{1 - \eta\gamma} \right\|_2 = \frac{1}{1 - \eta\gamma}.$$

Third, since  $\mathbf{H} = \mathbf{P}_{\mathbf{x}^*}^\perp (\mathbf{I}_n - \eta \mathbf{A}^\top \mathbf{A}) \mathbf{P}_{\mathbf{x}^*}^\perp / (1 - \eta\gamma)$  is symmetric, one can choose  $\mathbf{Q}$  in the eigendecomposition  $\mathbf{H} = \mathbf{Q}\mathbf{\Lambda}\mathbf{Q}^{-1}$  to be orthogonal, with  $\kappa(\mathbf{Q}) = 1$ . Thus, from (12), we obtain the region of linear convergence as

$$\|\mathbf{x} - \mathbf{x}^*\| \leq \frac{1 - \rho}{2(t^2 + t)}, \quad (53)$$

where  $t = \|\mathbf{I}_n - \eta \mathbf{A}^\top \mathbf{A}\|_2 / (1 - \eta\gamma)$ .

**Remark 6.** The local linear rate in (50) matches the rate provided by Theorem 1 in [35]. Compared to the setting in [35], here we consider a special case of the quadratic that is convex (and hence,  $\lambda_d \geq 0$ ). By minimizing the rate in (50) over  $\eta$ , we also obtain the same optimal rate of linear convergence given by Lemma 5 in [35]:

$$\rho_{opt} = \frac{\lambda_1 - \lambda_{n-1}}{\lambda_1 + \lambda_{n-1} - 2\gamma} \text{ with } \eta_{opt} = \frac{2}{\lambda_1 + \lambda_{n-1}}.$$

Interestingly, condition (51) implies  $\mathbf{x}^*$  is a strict local minimum of (46) (see Lemma 2 in [35]). Since  $\rho < 1$  is one of the conditions in Theorem 1, our analysis requires  $\mathbf{x}^*$  to be a strict local minimum of (46) in order to obtain linear convergence. Finally, our framework provides the region of linear convergence in (53), which is not given in [35].

## D. Matrix Completion

1) *Background:* The last application is an application of our framework to the matrix case. In matrix completion [61], given a rank- $r$  matrix  $\mathbf{M} \in \mathbb{R}^{m \times n}$  (for  $1 \leq r \leq \min\{m, n\}$ ) with a set of its observed entries indexed by  $\Omega$ , of cardinality  $0 < s < mn$ , we wish to recover the unknown entries of  $\mathbf{M}$  in the complement set  $\bar{\Omega}$  by solving the following optimization:

$$\min_{\mathbf{X} \in \mathbb{R}^{m \times n}} \frac{1}{2} \|\mathcal{P}_\Omega(\mathbf{X} - \mathbf{M})\|_F^2 \text{ s.t. } \text{rank}(\mathbf{X}) \leq r, \quad (54)$$

where  $\mathcal{P}_\Omega : \mathbb{R}^{m \times n} \rightarrow \mathbb{R}^{m \times n}$  is the orthogonal projection onto the set of  $m \times n$  matrices supported in  $\Omega$ , i.e.,

$$[\mathcal{P}_\Omega(\mathbf{X})]_{ij} = \begin{cases} X_{ij} & \text{if } (i, j) \in \Omega, \\ 0 & \text{if } (i, j) \notin \Omega. \end{cases}$$

It is noted that while  $\mathbf{M}$  is unknown, the projection  $\mathcal{P}_\Omega(\mathbf{M})$  is unambiguously determined by the observed entries in  $\mathbf{M}$ . In the literature, the PGD algorithm for solving (54) is also known as the Singular Value Projection (SVP) algorithm for matrix completion [12], with the update

$$\mathbf{X}^{(k+1)} = \mathcal{P}_{\mathcal{M}_{\leq r}}(\mathbf{X}^{(k)} - \eta \mathcal{P}_\Omega(\mathbf{X}^{(k)} - \mathbf{M})).$$

Here,  $\mathcal{M}_{\leq r}$  is the set of matrices of rank at most  $r$ , i.e.,

$$\mathcal{M}_{\leq r} = \{\mathbf{X} \in \mathbb{R}^{m \times n} \mid \text{rank}(\mathbf{X}) \leq r\}.$$

In addition, the orthogonal projection  $\mathcal{P}_{\mathcal{M}_{\leq r}} : \mathbb{R}^{m \times n} \rightarrow \mathcal{M}_{\leq r}$  is defined by Eckart–Young–Mirsky theorem [62] as follows. Let  $\text{SVD}(\mathbf{X})$  be the set of all triples  $(\mathbf{\Sigma}, \mathbf{U}, \mathbf{V})$  such that  $\mathbf{X} = \mathbf{U}\mathbf{\Sigma}\mathbf{V}^\top$  and

$$\begin{cases} \mathbf{\Sigma} = \text{diag}(\sigma_1(\mathbf{X}), \dots, \sigma_n(\mathbf{X})), \\ \mathbf{U} \in \mathbb{R}^{m \times n}, \mathbf{V} \in \mathbb{R}^{n \times n} : \mathbf{U}^\top \mathbf{U} = \mathbf{V}^\top \mathbf{V} = \mathbf{I}_n. \end{cases}$$

Denote  $\mathbf{u}_i(\mathbf{X})$  and  $\mathbf{v}_i(\mathbf{X})$  the  $i$ th columns of  $\mathbf{U}$  and  $\mathbf{V}$ , respectively. Then, the set of all projections of  $\mathbf{X}$  onto  $\mathcal{M}_{\leq r}$  is given by

$$\Pi_{\mathcal{M}_{\leq r}}(\mathbf{X}) = \left\{ \sum_{i=1}^r \sigma_i(\mathbf{X}) \mathbf{u}_i(\mathbf{X}) \mathbf{v}_i(\mathbf{X})^\top \mid (\mathbf{\Sigma}, \mathbf{U}, \mathbf{V}) \in \text{SVD}(\mathbf{X}) \right\}. \quad (55)$$

The set  $\Pi_{\mathcal{M}_{\leq r}}(\mathbf{X})$  is singleton if and only if  $\sigma_r(\mathbf{X}) = 0$  or  $\sigma_r(\mathbf{X}) > \sigma_{r+1}(\mathbf{X})$ . In the case  $\Pi_{\mathcal{M}_{\leq r}}(\mathbf{X})$  has multiple elements, we define  $\mathcal{P}_{\mathcal{M}_{\leq r}}(\mathbf{X})$  as the greatest element in  $\Pi_{\mathcal{M}_{\leq r}}(\mathbf{X})$  based on the lexicographical order. We re-emphasize that our subsequent analysis holds independently of this choice.

In differential geometry, it is well-known that  $\mathcal{M}_{\leq r}$  is a closed set of  $\mathbb{R}^{m \times n}$  but non-smooth in those points of rank strictly less than  $r$  [63]. Similar to sparse recovery, the smooth part of  $\mathcal{M}_{\leq r}$  is the set of matrices of fixed rank  $r$ :

$$\mathcal{M}_{=r} = \{\mathbf{X} \in \mathbb{R}^{m \times n} \mid \text{rank}(\mathbf{X}) = r\}.$$

At any  $\mathbf{X}^* \in \mathcal{M}_{=r}$ , it is shown [64] that derivative of  $\mathcal{P}_{\mathcal{M}_{\leq r}}$  is a linear mapping from  $\mathbb{R}^{m \times n}$  to  $\mathbb{R}^{m \times n}$  satisfying

$$\nabla \mathcal{P}_{\mathcal{M}_{\leq r}}(\mathbf{X}^*)(\mathbf{\Delta}) = \mathbf{\Delta} - \mathbf{P}_{\mathbf{U}_\perp} \mathbf{\Delta} \mathbf{P}_{\mathbf{V}_\perp}, \quad (56)$$

where  $P_{U_\perp}$  and  $P_{V_\perp}$  are the projections onto the left and right null spaces of  $\mathbf{X}^*$ , respectively. More importantly, for any  $\Delta \in \mathbb{R}^{m \times n}$ , Theorem 3 in [64] asserts that

$$\sup_{\mathbf{Y} \in \Pi_{\mathcal{M}_{\leq r}}(\mathbf{X}^* + \Delta)} \|\mathbf{Y} - \mathbf{X}^* - \nabla \mathcal{P}_{\mathcal{M}_{\leq r}}(\mathbf{X}^*)(\Delta)\|_F \leq 4(1 + \sqrt{2})\|\Delta\|_F^2. \quad (57)$$

2) *Vectorized version of matrix completion:* To apply our proposed framework to matrix completion, we consider a vectorized version of (54) as follows. Slightly extending the notation, we denote  $\text{vec}(\mathcal{M}_{\leq r}) = \{\text{vec}(\mathbf{X}) \mid \mathbf{X} \in \mathcal{M}_{\leq r}\}$  and  $\text{vec}(\Omega) = \{(j-1)m+i \mid (i,j) \in \Omega\}$  with  $s$  distinct elements  $1 \leq i_1 < \dots < i_s \leq mn$ . Let  $\mathbf{S}_\Omega = [e_{i_1}, \dots, e_{i_s}] \in \mathbb{R}^{mn \times s}$  be the selection matrix satisfying

$$\begin{cases} \mathbf{S}_\Omega^\top \mathbf{S}_\Omega = \mathbf{I}_s, \\ \text{vec}(\mathcal{P}_\Omega(\mathbf{X})) = \mathbf{S}_\Omega \mathbf{S}_\Omega^\top \text{vec}(\mathbf{X}). \end{cases}$$

Then, problem (54) can be represented as

$$\min_{\mathbf{x} \in \mathbb{R}^{mn}} \frac{1}{2} \|\mathbf{S}_\Omega \mathbf{S}_\Omega^\top \mathbf{x} - \mathbf{S}_\Omega \mathbf{S}_\Omega^\top \text{vec}(\mathbf{M})\|^2 \text{ s.t. } \mathbf{x} \in \text{vec}(\mathcal{M}_{\leq r}).$$

**Step 1:** In this vectorized version of matrix completion, we have  $\mathbf{A} = \mathbf{S}_\Omega \mathbf{S}_\Omega^\top$ ,  $\mathbf{b} = \mathbf{S}_\Omega \mathbf{S}_\Omega^\top \text{vec}(\mathbf{M})$ , and  $\mathcal{C} = \text{vec}(\mathcal{M}_{\leq r})$  is a closed non-convex set. For any vector  $\mathbf{x} \in \mathbb{R}^{mn}$ , let  $\mathbf{X} = \text{vec}^{-1}(\mathbf{x})$  with  $\mathcal{P}_{\mathcal{M}_{\leq r}}(\mathbf{X}) = \sum_{i=1}^r \sigma_i(\mathbf{X}) \mathbf{u}_i(\mathbf{X}) \mathbf{v}_i(\mathbf{X})^\top$ , for some  $(\Sigma, \mathbf{U}, \mathbf{V}) \in \text{SVD}(\mathbf{X})$ . The projection  $\mathcal{P}_\mathcal{C}$  is given by  $\mathcal{P}_\mathcal{C}(\mathbf{x}) = \text{vec}(\sum_{i=1}^r \sigma_i(\mathbf{X}) \mathbf{u}_i(\mathbf{X}) \mathbf{v}_i(\mathbf{X})^\top)$ . Using the fact that  $\text{vec}(\mathbf{u}\mathbf{v}^\top) = \mathbf{v} \otimes \mathbf{u}$ , for any vectors  $\mathbf{u}$  and  $\mathbf{v}$  of compatible dimensions,  $\mathcal{P}_\mathcal{C}$  can then be represented as

$$\mathcal{P}_\mathcal{C}(\mathbf{x}) = \sum_{i=1}^r \sigma_i(\mathbf{X}) (\mathbf{v}_i(\mathbf{X}) \otimes \mathbf{u}_i(\mathbf{X})). \quad (58)$$

**Step 2:** In the following, we show that  $\mathcal{P}_\mathcal{C}$  is Lipschitz-continuously differentiable at any

$$\mathbf{x}^* \in \text{vec}(\mathcal{M}_{=r}) = \{\text{vec}(\mathbf{X}) \mid \mathbf{X} \in \mathcal{M}_{=r}\},$$

with

$$\nabla \mathcal{P}_\mathcal{C}(\mathbf{x}^*) = \mathbf{P}_{U_\perp V_\perp}^\perp, \quad c_1(\mathbf{x}^*) = \infty, \quad c_2(\mathbf{x}^*) = 4(1 + \sqrt{2}).$$

The constants  $c_1(\mathbf{x}^*)$  and  $c_2(\mathbf{x}^*)$  are obtained from (57). Regarding  $\nabla \mathcal{P}_\mathcal{C}(\mathbf{x}^*)$ , let  $\mathbf{P}_{U_\perp}$  and  $\mathbf{P}_{V_\perp}$  be the projections onto the left and right null spaces of  $\mathbf{X}^* = \text{vec}^{-1}(\mathbf{x}^*)$ , respectively. Denote  $\mathbf{P}_{U_\perp V_\perp}^\perp = \mathbf{P}_{V_\perp}^\perp \otimes \mathbf{P}_{U_\perp}^\perp$  and  $\mathbf{P}_{U_\perp V_\perp}^\perp = \mathbf{I}_{mn} - \mathbf{P}_{U_\perp V_\perp}$ . Since  $\text{vec}(\mathbf{A}\mathbf{B}\mathbf{C}) = (\mathbf{C}^\top \otimes \mathbf{A}) \text{vec}(\mathbf{B})$ , for any matrices  $\mathbf{A}$ ,  $\mathbf{B}$ , and  $\mathbf{C}$  of compatible dimensions, (56) can be vectorized to obtain  $\nabla \mathcal{P}_\mathcal{C}(\mathbf{x}^*)(\delta) = (\mathbf{I}_{mn} - \mathbf{P}_{V_\perp}^\perp \otimes \mathbf{P}_{U_\perp}^\perp) \delta = \mathbf{P}_{U_\perp V_\perp}^\perp \delta$  for any  $\delta \in \mathbb{R}^{mn}$ .

Next, the stationarity equation (7) can be represented using  $\nabla \mathcal{P}_\mathcal{C}(\mathbf{x}^*)(\delta) = \mathbf{P}_{U_\perp V_\perp}^\perp \delta$  as  $\mathbf{P}_{U_\perp V_\perp}^\perp \cdot \mathbf{S}_\Omega \mathbf{S}_\Omega^\top (\mathbf{S}_\Omega \mathbf{S}_\Omega^\top \mathbf{x}^* - \mathbf{S}_\Omega \mathbf{S}_\Omega^\top \text{vec}(\mathbf{M})) = \mathbf{0}$ . Denote  $\mathbf{Q}_\perp \in \mathbb{R}^{mn \times r(m+n-r)}$  the matrix satisfying  $\mathbf{Q}_\perp^\top \mathbf{Q}_\perp = \mathbf{I}_{r(m+n-r)}$  and  $\mathbf{Q}_\perp \mathbf{Q}_\perp^\top = \mathbf{P}_{U_\perp V_\perp}^\perp$ . Then, we obtain the conditions for  $\mathbf{x}^*$  to be a Lipschitz stationary point of (54) are  $\mathbf{x}^* \in \text{vec}(\mathcal{M}_{=r})$  and

$$\mathbf{Q}_\perp^\top \mathbf{S}_\Omega \mathbf{S}_\Omega^\top (\mathbf{x}^* - \text{vec}(\mathbf{M})) = \mathbf{0}. \quad (59)$$

**Step 3:** Generally, analyzing the Lipschitz-continuous differentiability of the projection  $\mathcal{P}_\mathcal{C}$  in (58) at  $\mathbf{x} \notin \text{vec}(\mathcal{M}_{=r})$  is

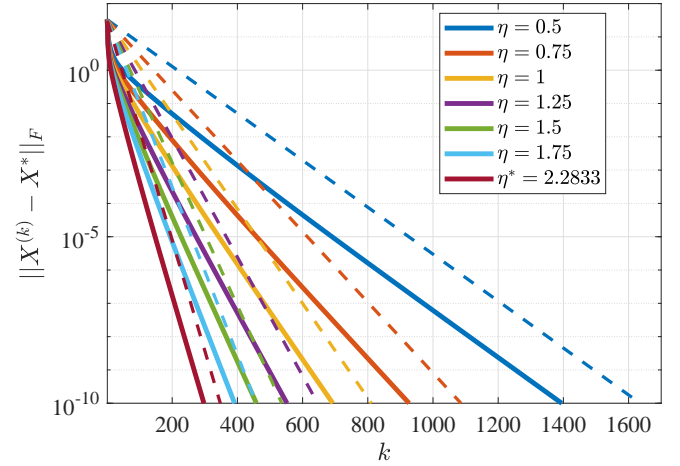


Fig. 2: Projected gradient descent with various step sizes for solving matrix completion with  $m = 50, n = 40, r = 3$ , and  $s = 800$ . The figure compares the log-scale distance to the solution as a function of the number of iterations (solid lines) with the corresponding theoretical rate of linear convergence given by (61) (dashed lines) up to a constant.  $\eta^*$  is the optimal step size given by (63).

non-trivial and beyond the scope of this manuscript. For the purpose of demonstration, we restrict our subsequent analysis to the Lipschitz stationary point  $\mathbf{x}^* \in \text{vec}(\mathcal{M}_{=r})$  satisfying

$$\mathbf{S}_\Omega^\top (\mathbf{x}^* - \text{vec}(\mathbf{M})) = \mathbf{0}. \quad (60)$$

Intuitively, this assumption means the corresponding matrix  $\mathbf{X}^*$  is an exact solution of (54), i.e.,  $\mathcal{P}_\Omega(\mathbf{X}^*) = \mathcal{P}_\Omega(\mathbf{M})$ . From (60), for any  $\eta > 0$ , we have

$$\mathbf{z}_\eta^* = \mathbf{x}^* - \eta \mathbf{S}_\Omega \mathbf{S}_\Omega^\top (\mathbf{x}^* - \text{vec}(\mathbf{M})) = \mathbf{x}^*.$$

Thus,  $\mathcal{P}_\mathcal{C}$  is Lipschitz-continuously differentiable at  $\mathbf{z}_\eta^*$  with

$$\nabla \mathcal{P}_\mathcal{C}(\mathbf{z}_\eta^*) = \mathbf{P}_{U_\perp V_\perp}^\perp, \quad c_1(\mathbf{z}_\eta^*) = \infty, \quad c_2(\mathbf{z}_\eta^*) = 4(1 + \sqrt{2}).$$

**Step 4:** Since  $\nabla \mathcal{P}_\mathcal{C}(\mathbf{z}_\eta^*) = \nabla \mathcal{P}_\mathcal{C}(\mathbf{x}^*) = \mathbf{P}_{U_\perp V_\perp}^\perp$ , using (18), we obtain the asymptotic linear rate as

$$\rho = \max\{|1 - \eta \lambda_1|, |1 - \eta \lambda_{r(m+n-r)}|\}, \quad (61)$$

where  $\lambda_1$  and  $\lambda_{r(m+n-r)}$  are the largest and smallest eigenvalues of  $\mathbf{Q}_\perp^\top \mathbf{S}_\Omega \mathbf{S}_\Omega^\top \mathbf{Q}_\perp$ , respectively.

**Step 5:** From (61), we have  $\rho < 1$  if and only if  $\mathbf{Q}_\perp^\top \mathbf{S}_\Omega \mathbf{S}_\Omega^\top \mathbf{Q}_\perp$  has full rank and

$$0 < \eta < \frac{2}{\|\mathbf{Q}_\perp^\top \mathbf{S}_\Omega \mathbf{S}_\Omega^\top \mathbf{Q}_\perp\|_2}.$$

**Step 6:** Recall that  $c_1(\mathbf{x}^*) = c_1(\mathbf{z}_\eta^*) = \infty$ . Since  $\nabla \mathcal{P}_\mathcal{C}(\mathbf{z}_\eta^*) = \nabla \mathcal{P}_\mathcal{C}(\mathbf{x}^*) = \mathbf{P}_{U_\perp V_\perp}^\perp$ , using (19), the region of linear convergence is given by

$$\|\mathbf{x} - \mathbf{x}^*\| \leq \frac{1 - \rho}{8(1 + \sqrt{2})}. \quad (62)$$

**Remark 7.** Similar to (37) and (38), the optimal step size and the optimal convergence rate are given by

$$\eta_{opt} = \frac{2}{\lambda_1(\mathbf{Q}_\perp^\top \mathbf{S}_\Omega \mathbf{S}_\Omega^\top \mathbf{Q}_\perp) + \lambda_{r(m+n-r)}(\mathbf{Q}_\perp^\top \mathbf{S}_\Omega \mathbf{S}_\Omega^\top \mathbf{Q}_\perp)},$$

$$\rho_{opt} = 1 - \frac{2}{\kappa(\mathbf{Q}_\perp^\top \mathbf{S}_\Omega \mathbf{S}_\Omega^\top \mathbf{Q}_\perp) + 1}. \quad (63)$$

Figure 2 depicts the agreement between the established rate in (61) and the empirical rate observed by performing PGD with various step sizes. The data is generated randomly as follows. First, we sample two matrices  $\mathbf{A}$  and  $\mathbf{B}$  with i.i.d normally distributed entries, of dimensions  $m \times r$  and  $n \times r$ , respectively. Next, we obtain the rank- $r$  matrix of dimension  $m \times n$  as the product  $\mathbf{X}^* = \mathbf{A}\mathbf{B}^\top$ . Third, we select the observation  $\Omega$  uniformly at random among the  $mn$  positions in  $\mathbf{X}^*$ . It can be seen from Fig. 2 that the theoretical rate matches well the empirical rate, reassuring the correctness of our analysis in the previous section.

**Remark 8.** The rate in (61) has not been proposed in the literature. However, in the special case of using unit step size, it matches the rate established for the IHTSVD algorithm in [32]. In their work, the authors provide the result relative to the matrix  $(\mathbf{S}_\Omega)^\top \mathbf{P}_{\mathbf{U}_\perp \mathbf{V}_\perp} \mathbf{S}_\Omega$  instead of  $\mathbf{Q}_\perp^\top \mathbf{S}_\Omega \mathbf{S}_\Omega^\top \mathbf{Q}_\perp$ , where  $\mathbf{S}_\Omega \in \mathbb{R}^{mn \times (mn-s)}$  is the selection matrix that is complement to  $\mathbf{S}_\Omega$ . It can be shown that the two matrices share the same set of eigenvalues while may only differ by the eigenvalues at 1. Since IHTSVD uses  $\eta = 1$ , these unit eigenvalues do not affect the maximization in (61). Compared to the local convergence result in [32], our application in this subsection not only considers PGD with different step sizes but also includes the region of linear convergence in (62).

## VI. CONCLUSION

We presented a unified framework to analyze the local convergence of projected gradient descent for constrained least squares. Our analysis provides sufficient conditions for linear convergence, the asymptotic rate of convergence in a closed-form expression, and the number of iterations required to reach certain accuracy. Notably, our technique relies on the Lipschitz-continuous differentiability of the projection operator at two key points:  $\mathbf{x}^*$  and  $\mathbf{z}_\eta^*$ . By viewing the projection update as a fixed-point iteration, this idea can also be extended to analyze other variants of projected gradient descent such as alternating projection, gradient descent with implicit constraints, and accelerated methods. Finally, we demonstrated the application of our proposed framework to local convergence analysis of projected gradient descent in four well-known problems in machine learning and signal processing.

## APPENDIX A PROOF OF EXAMPLE 1

Our goal in this proof is to establish the Lipschitz differentiability of the projection operator onto the unit sphere  $\mathcal{C} = \{\mathbf{x} \in \mathbb{R}^n \mid \|\mathbf{x}\| = 1\}$ . We start by establishing the Lipschitz differentiability at a point on  $\mathcal{C}$  and then extend it to any nonzero point in  $\mathbb{R}^n$ . For the Lipschitz differentiability on  $\mathcal{C}$ , we introduce the following lemma:

**Lemma 5.** For any  $\mathbf{x}^* \in \mathcal{C}$ , we have

$$\sup_{\mathbf{y} \in \Pi_{\mathcal{C}}(\mathbf{x}^* + \delta)} \|\mathbf{y} - \mathbf{x}^* - (\mathbf{I} - \mathbf{x}^*(\mathbf{x}^*)^\top) \delta\| \leq 2\|\delta\|^2. \quad (64)$$

*Proof.* We consider two cases:

- If  $\mathbf{x}^* + \delta = \mathbf{0}$ , then  $\Pi_{\mathcal{C}}(\mathbf{0}) = \mathcal{C}$  and  $\|\delta\| = \|\mathbf{x}^*\| = 1$ . For any  $\mathbf{y} \in \mathcal{C}$ , substituting  $\delta = -\mathbf{x}^*$  and then using the fact that  $\mathbf{I} - \mathbf{x}^*(\mathbf{x}^*)^\top$  is the projection onto the null space of  $\mathbf{x}^*$ , we have

$$\begin{aligned} \mathbf{y} - \mathbf{x}^* - (\mathbf{I} - \mathbf{x}^*(\mathbf{x}^*)^\top) \delta &= \mathbf{y} - \mathbf{x}^* + (\mathbf{I} - \mathbf{x}^*(\mathbf{x}^*)^\top) \mathbf{x}^* \\ &= \mathbf{y} - \mathbf{x}^*. \end{aligned}$$

Next, taking the norm and using the triangle inequality yield

$$\begin{aligned} \|\mathbf{y} - \mathbf{x}^* - (\mathbf{I} - \mathbf{x}^*(\mathbf{x}^*)^\top) \delta\| &= \|\mathbf{y} - \mathbf{x}^*\| \\ &\leq \|\mathbf{y}\| + \|\mathbf{x}^*\| = 2\|\delta\|^2, \end{aligned}$$

where the last step stems from  $\|\mathbf{y}\| = \|\mathbf{x}^*\| = \|\delta\| = 1$ . Thus, (64) holds in this case.

- If  $\mathbf{x}^* + \delta \neq \mathbf{0}$ , then  $\Pi_{\mathcal{C}}(\mathbf{x}^* + \delta)$  is singleton containing the unique projection

$$\mathcal{P}_{\mathcal{C}}(\mathbf{x}^* + \delta) = \frac{\mathbf{x}^* + \delta}{\|\mathbf{x}^* + \delta\|}.$$

Hence, (64) is equivalent to

$$\left\| \frac{\mathbf{x}^* + \delta}{\|\mathbf{x}^* + \delta\|} - \mathbf{x}^* - (\mathbf{I} - \mathbf{x}^*(\mathbf{x}^*)^\top) \delta \right\| \leq 2\|\delta\|^2. \quad (65)$$

We prove (65) by (i) showing that for any scalars  $u > 0$  and  $(1-u)^2 \leq v \leq (1+u)^2$ :

$$(17u-2)v^2 - 2u(1-u)^2v + (1-u)^4(u+2) \geq 0, \quad (66)$$

and (ii) showing that (66) is equivalent to (65) with  $u = \|\mathbf{x}^* + \delta\| > 0$  and  $v = \|\delta\|^2 \geq 0$ .

(i) To prove (66), let us consider the following cases:

- 1) If  $0 < u \leq 2/17$ , then for  $v \leq (1+u)^2$ , we have

$$\begin{aligned} (17u-2)v^2 - 2u(1-u)^2v + (1-u)^4(u+2) &\geq (17u-2)(1+u)^4 - 2u(1-u)^2(1+u)^2 \\ &\quad + (1-u)^4(u+2) \\ &= 16u^2(u+2)(u^2+2u+2) \geq 0. \end{aligned}$$

- 2) If  $2/17 < u \leq 1/2$ , then for  $(1-u)^2 \leq v \leq (1+u)^2$ , the following holds

$$\begin{aligned} (17u-2)v^2 - 2u(1-u)^2v + (1-u)^4(u+2) &\geq (17u-2)(1-u)^4 - 2u(1-u)^2(1+u)^2 \\ &\quad + (1-u)^4(u+2) \\ &= 8u(1-u)^2(2-u)(1-2u) \geq 0. \end{aligned}$$

- 3) If  $u > 1/2$ , using the quadratic vertex at  $v = u(1-u)^2/(17u-2)$  as the minimum point, we obtain

$$\begin{aligned} (17u-2)v^2 - 2u(1-u)^2v + (1-u)^4(u+2) &\geq \frac{4(1-u)^4(4u^2+8u-1)}{17u-2} \geq 0. \end{aligned}$$

(ii) Now for  $u = \|\mathbf{x}^* + \boldsymbol{\delta}\| > 0$  and  $v = \|\boldsymbol{\delta}\|^2 \geq 0$ , we have  $(\mathbf{x}^*)^\top \boldsymbol{\delta} = (u^2 - v - 1)/2$  and

$$\begin{aligned}
(65) &\Leftrightarrow \left\| \frac{\mathbf{x}^* + \boldsymbol{\delta}}{\|\mathbf{x}^* + \boldsymbol{\delta}\|} - \mathbf{x}^* - (\mathbf{I} - \mathbf{x}^*(\mathbf{x}^*)^\top) \boldsymbol{\delta} \right\| \leq 2\|\boldsymbol{\delta}\|^2 \\
&\Leftrightarrow \|\mathbf{x}^* + \boldsymbol{\delta} - \|\mathbf{x}^* + \boldsymbol{\delta}\|(\mathbf{x}^* + \boldsymbol{\delta} - \mathbf{x}^*(\mathbf{x}^*)^\top \boldsymbol{\delta})\|^2 \\
&\quad \leq 4\|\mathbf{x}^* + \boldsymbol{\delta}\|^2 \|\boldsymbol{\delta}\|^4 \\
&\Leftrightarrow \|(1-u)(\mathbf{x}^* + \boldsymbol{\delta}) + u((\mathbf{x}^*)^\top \boldsymbol{\delta})\mathbf{x}^*\|_2^2 \leq 4u^2v^2 \\
&\Leftrightarrow (1-u)^2u^2 + u^2\left(\frac{u^2-v-1}{2}\right)^2 \\
&\quad + 2u(1-u)\frac{u^2-v-1}{2}\frac{u^2-v+1}{2} \leq 4u^2v^2 \\
&\Leftrightarrow (66).
\end{aligned}$$

Finally, by the triangle inequality, we have

$$\|\|\mathbf{x}^* + \boldsymbol{\delta}\| - \|\mathbf{x}^*\|\| \leq \|\boldsymbol{\delta}\| \leq \|\mathbf{x}^*\| + \|\mathbf{x}^* + \boldsymbol{\delta}\|,$$

which in turn verifies  $(1-u)^2 \leq v \leq (1+u)^2$ .

This completes our proof of the lemma.  $\square$

Next, to extend the result in Lemma 5 to any  $\mathbf{x} \in \mathbb{R} \setminus \{0\}$ , we substitute  $\mathbf{x}^* = \mathbf{x}/\|\mathbf{x}\|$  and  $\boldsymbol{\delta} = \boldsymbol{\delta}/\|\mathbf{x}\|$  into (64) and obtain

$$\sup_{\mathbf{y} \in \Pi_C\left(\frac{\mathbf{x}}{\|\mathbf{x}\|} + \frac{\boldsymbol{\delta}}{\|\mathbf{x}\|}\right)} \left\| \mathbf{y} - \frac{\mathbf{x}}{\|\mathbf{x}\|} - \left(\mathbf{I}_n - \frac{\mathbf{x}\mathbf{x}^\top}{\|\mathbf{x}\|^2}\right) \frac{\boldsymbol{\delta}}{\|\mathbf{x}\|} \right\| \leq 2\frac{\|\boldsymbol{\delta}\|^2}{\|\mathbf{x}\|^2}. \quad (67)$$

Since the projection onto the unit sphere is scale-invariant,

$$\Pi_C\left(\frac{\mathbf{x}}{\|\mathbf{x}\|} + \frac{\boldsymbol{\delta}}{\|\mathbf{x}\|}\right) = \Pi_C(\mathbf{x} + \boldsymbol{\delta}). \quad (68)$$

Substituting (68) into (67) yields (5). Thus, by Definition 1, for any  $\mathbf{x} \neq \mathbf{0}$  we obtain

$$\begin{aligned}
\nabla \mathcal{P}_C(\mathbf{x}) &= \frac{1}{\|\mathbf{x}\|} \left(\mathbf{I}_n - \frac{\mathbf{x}\mathbf{x}^\top}{\|\mathbf{x}\|^2}\right), \\
c_1(\mathbf{x}) &= \infty, \quad c_2(\mathbf{x}) = \frac{2}{\|\mathbf{x}\|^2}.
\end{aligned}$$

As a closing remark, the choice of  $c_1(\mathbf{x})$  and  $c_2(\mathbf{x})$  in Definition 1 is not unique. Specifically, for any  $\mathbf{x} \neq \mathbf{0}$  and  $\boldsymbol{\delta} \in \mathbb{R}^n$ , the second-order directional derivative is given by

$$\nabla^2 \mathcal{P}_C(\mathbf{x})(\boldsymbol{\delta}, \boldsymbol{\delta}) = \left(\frac{3}{2}\left(\frac{\boldsymbol{\delta}^\top \mathbf{x}}{\|\mathbf{x}\|^2}\right)^2 \mathbf{I} - \frac{1}{2}\frac{\|\boldsymbol{\delta}\|^2}{\|\mathbf{x}\|^2} \mathbf{I} - \frac{\boldsymbol{\delta}\boldsymbol{\delta}^\top}{\|\mathbf{x}\|^2}\right) \frac{\mathbf{x}}{\|\mathbf{x}\|}.$$

Using  $t = (\mathbf{x}^\top \boldsymbol{\delta})/(\|\mathbf{x}\| \cdot \|\boldsymbol{\delta}\|)$ , the last equation can be rewritten as

$$\nabla^2 \mathcal{P}_C(\mathbf{x})(\boldsymbol{\delta}, \boldsymbol{\delta}) = \frac{\|\boldsymbol{\delta}\|^2}{\|\mathbf{x}\|^2} \left(\frac{3}{2}t^2 - \frac{1}{2}\right) \frac{\mathbf{x}}{\|\mathbf{x}\|} - t \frac{\boldsymbol{\delta}}{\|\boldsymbol{\delta}\|}.$$

Taking the norm and simplifying, we have

$$\|\nabla^2 \mathcal{P}_C(\mathbf{x})(\boldsymbol{\delta}, \boldsymbol{\delta})\| = \frac{\|\boldsymbol{\delta}\|^2}{\|\mathbf{x}\|^2} \sqrt{\frac{1+2t^2-3t^4}{4}} \leq \frac{1}{\sqrt{3}\|\mathbf{x}\|^2} \|\boldsymbol{\delta}\|^2,$$

where the last inequality becomes an equality if  $t = \pm 1/\sqrt{3}$ . Therefore, by decreasing  $c_1(\mathbf{x}) \rightarrow 0$ , we can choose smaller  $c_2(\mathbf{x})$  as  $c_2(\mathbf{x})$  approaches  $1/(\sqrt{3}\|\mathbf{x}\|^2)$ . As it can be seen later, the choice of  $c_1(\mathbf{x})$  and  $c_2(\mathbf{x})$  affects the region of linear convergence in (12).

## APPENDIX B PROOF OF LEMMA 1

Our goal in the proof of Lemma 1 is to show that if the fixed point condition  $\mathbf{x}^* = \mathcal{P}_C(\mathbf{x}^* - \eta \mathbf{A}^\top(\mathbf{A}\mathbf{x}^* - \mathbf{b}))$  holds, then the stationarity condition  $\nabla \mathcal{P}_C(\mathbf{x}^*) \cdot \mathbf{A}^\top(\mathbf{A}\mathbf{x}^* - \mathbf{b}) = \mathbf{0}$  holds. Note that if  $\mathbf{A}^\top(\mathbf{A}\mathbf{x}^* - \mathbf{b}) = \mathbf{0}$ , then the stationarity condition holds trivially. Hence, we focus on the proof for  $\mathbf{A}^\top(\mathbf{A}\mathbf{x}^* - \mathbf{b}) \neq \mathbf{0}$ . We first show that for any  $0 \leq \alpha < 1$ ,  $\mathbf{x}^* = \mathcal{P}_C(\mathbf{x}^* - \eta \mathbf{A}^\top(\mathbf{A}\mathbf{x}^* - \mathbf{b}))$  is a sufficient condition for

$$\Pi_C(\mathbf{x}^* - \alpha \eta \mathbf{A}^\top(\mathbf{A}\mathbf{x}^* - \mathbf{b})) = \{\mathbf{x}^*\}. \quad (69)$$

Then, using (69) and the differentiability of  $\mathcal{P}_C$  at  $\mathbf{x}^*$ , we prove that  $\nabla \mathcal{P}_C(\mathbf{x}^*) \cdot \mathbf{A}^\top(\mathbf{A}\mathbf{x}^* - \mathbf{b}) = \mathbf{0}$ . We proceed with the detailed proof.

First, let  $\mathbf{v}^* = \mathbf{A}^\top(\mathbf{A}\mathbf{x}^* - \mathbf{b})$  and  $\mathbf{z}_{\alpha\eta}^* = \mathbf{x}^* - \alpha \eta \mathbf{v}^*$ . On the one hand, for any  $0 \leq \alpha < 1$  and  $\mathbf{y} \in \Pi_C(\mathbf{z}_{\alpha\eta}^*)$ , we have

$$\begin{aligned}
\|\mathbf{y} - \mathbf{z}_{\alpha\eta}^*\| &= \|(\mathbf{y} - \mathbf{z}_{\alpha\eta}^*) + (\mathbf{z}_{\alpha\eta}^* - \mathbf{z}_{\eta}^*)\| \\
&\leq \|\mathbf{y} - \mathbf{z}_{\alpha\eta}^*\| + \|\mathbf{z}_{\alpha\eta}^* - \mathbf{z}_{\eta}^*\| \\
&= d(\mathbf{z}_{\alpha\eta}^*, \mathcal{C}) + \|\mathbf{z}_{\alpha\eta}^* - \mathbf{z}_{\eta}^*\| \\
&\leq \|\mathbf{x}^* - \mathbf{z}_{\alpha\eta}^*\| + \|\mathbf{z}_{\alpha\eta}^* - \mathbf{z}_{\eta}^*\|, \quad (70)
\end{aligned}$$

where the first inequality uses the triangle inequality that holds when  $\mathbf{y} - \mathbf{z}_{\alpha\eta}^* = \beta(\mathbf{z}_{\alpha\eta}^* - \mathbf{z}_{\eta}^*)$ , for some  $\beta \geq 0$ . Using the fact that  $\mathbf{z}_{\eta}^* = \mathbf{x}^* - \eta \mathbf{v}^*$  and  $\mathbf{z}_{\alpha\eta}^* = \mathbf{x}^* - \alpha \eta \mathbf{v}^*$ , we obtain

$$\begin{aligned}
\|\mathbf{x}^* - \mathbf{z}_{\alpha\eta}^*\| + \|\mathbf{z}_{\alpha\eta}^* - \mathbf{z}_{\eta}^*\| &= \|\alpha \eta \mathbf{v}^*\| + \|(1-\alpha)\eta \mathbf{v}^*\| \\
&= \|\alpha \eta \mathbf{v}^*\| + \|(1-\alpha)\eta \mathbf{v}^*\| \\
&= \|\eta \mathbf{v}^*\| = \|\mathbf{x}^* - \mathbf{z}_{\eta}^*\|. \quad (71)
\end{aligned}$$

From (70) and (71), we have

$$\|\mathbf{y} - \mathbf{z}_{\eta}^*\| \leq \|\mathbf{x}^* - \mathbf{z}_{\eta}^*\|, \quad (72)$$

with the equality holding if and only if

$$\begin{cases} \mathbf{y} - \mathbf{z}_{\alpha\eta}^* = \beta(\mathbf{z}_{\alpha\eta}^* - \mathbf{z}_{\eta}^*), \\ \|\mathbf{y} - \mathbf{z}_{\alpha\eta}^*\| = \|\mathbf{x}^* - \mathbf{z}_{\alpha\eta}^*\|. \end{cases} \quad (73)$$

Using the fact that  $\mathbf{z}_{\eta}^* = \mathbf{x}^* - \eta \mathbf{v}^*$  and  $\mathbf{z}_{\alpha\eta}^* = \mathbf{x}^* - \alpha \eta \mathbf{v}^*$ , (73) holds if and only if

$$\begin{cases} \beta = \frac{\alpha}{1-\alpha}, \\ \mathbf{y} = \mathbf{x}^*. \end{cases} \quad (74)$$

On the other hand, since  $\mathbf{x}^* = \mathcal{P}_C(\mathbf{z}_{\eta}^*)$  and  $\mathbf{y} \in \mathcal{C}$ , we have

$$\|\mathbf{y} - \mathbf{z}_{\eta}^*\| \geq \|\mathbf{x}^* - \mathbf{z}_{\eta}^*\|. \quad (75)$$

From (72) and (75), we conclude that  $\|\mathbf{y} - \mathbf{z}_{\eta}^*\| = \|\mathbf{x}^* - \mathbf{z}_{\eta}^*\|$ . Moreover, from (74), the equality holds if and only if  $\mathbf{y} = \mathbf{x}^*$ . Since this holds for any  $\mathbf{y} \in \Pi_C(\mathbf{z}_{\alpha\eta}^*)$ , we conclude that  $\Pi_C(\mathbf{z}_{\alpha\eta}^*) = \{\mathbf{x}^*\}$  for all  $0 \leq \alpha < 1$ .

Next, using the differentiability of the projection  $\mathcal{P}_C$  at  $\mathbf{x}^*$  from Definition 1, we have

$$\lim_{\alpha \rightarrow 0} \sup_{\mathbf{y} \in \Pi_C(\mathbf{x}^* - \alpha \eta \mathbf{v}^*)} \frac{\|\mathbf{y} - \mathcal{P}_C(\mathbf{x}^*) - \nabla \mathcal{P}_C(\mathbf{x}^*)(\alpha \eta \mathbf{v}^*)\|}{\|\alpha \eta \mathbf{v}^*\|} = 0.$$

Substituting  $\Pi_C(\mathbf{x}^* - \alpha\eta\mathbf{v}^*) = \Pi_C(\mathbf{z}_{\alpha\eta}^*) = \{\mathbf{x}^*\}$  and  $\mathcal{P}_C(\mathbf{x}^*) = \mathbf{x}^*$  into the last equation, we obtain

$$\begin{aligned} 0 &= \lim_{\alpha \rightarrow 0} \frac{\|\mathbf{x}^* - \mathbf{x}^* - \alpha\eta\nabla\mathcal{P}_C(\mathbf{x}^*)\mathbf{v}^*\|}{\|\alpha\eta\mathbf{v}^*\|} \\ &= \lim_{\alpha \rightarrow 0} \frac{\alpha\eta\|\nabla\mathcal{P}_C(\mathbf{x}^*)\mathbf{v}^*\|}{\alpha\eta\|\mathbf{v}^*\|} \\ &= \frac{\|\nabla\mathcal{P}_C(\mathbf{x}^*)\mathbf{v}^*\|}{\|\mathbf{v}^*\|}, \end{aligned}$$

which only holds if  $\nabla\mathcal{P}_C(\mathbf{x}^*)\mathbf{v}^* = \mathbf{0}$ . This completes our proof of the lemma.

#### APPENDIX C PROOF OF COROLLARY 1

In the following, under the assumption  $\nabla\mathcal{P}_C(\mathbf{z}_\eta^*) = \nabla\mathcal{P}_C(\mathbf{x}^*) = \mathbf{U}_{\mathbf{x}^*}\mathbf{U}_{\mathbf{x}^*}^\top$ , we show that (i) the asymptotic convergence rate  $\rho(\mathbf{H})$  is given by (18), (ii) the sufficient conditions for  $\rho(\mathbf{H}) < 1$  are  $(\mathbf{A}\mathbf{U}_{\mathbf{x}^*})^\top\mathbf{A}\mathbf{U}_{\mathbf{x}^*}$  is full rank and (17) holds, and (iii) the region of linear convergence can be simplified from (12) to (19).

First, we prove (18) by simplifying the expression of  $\mathbf{H}$  in (16) and the fact that  $\mathbf{U}_{\mathbf{x}^*}^\top\mathbf{U}_{\mathbf{x}^*} = \mathbf{I}_d$  as follows. Substituting  $\nabla\mathcal{P}_C(\mathbf{x}^*)$  and  $\nabla\mathcal{P}_C(\mathbf{z}_\eta^*)$  by  $\mathbf{U}_{\mathbf{x}^*}\mathbf{U}_{\mathbf{x}^*}^\top$  into (11) yields

$$\begin{aligned} \mathbf{H} &= \mathbf{U}_{\mathbf{x}^*}\mathbf{U}_{\mathbf{x}^*}^\top(\mathbf{I}_n - \eta\mathbf{A}^\top\mathbf{A})\mathbf{U}_{\mathbf{x}^*}\mathbf{U}_{\mathbf{x}^*}^\top \\ &= \mathbf{U}_{\mathbf{x}^*}(\mathbf{I}_d - \eta\mathbf{U}_{\mathbf{x}^*}^\top\mathbf{A}^\top\mathbf{A}\mathbf{U}_{\mathbf{x}^*})\mathbf{U}_{\mathbf{x}^*}^\top, \end{aligned}$$

where the second equality stems from  $\mathbf{U}_{\mathbf{x}^*}^\top\mathbf{U}_{\mathbf{x}^*} = \mathbf{I}_d$ . Since  $\mathbf{H}$  is symmetric, its spectral radius equals to its spectral norm:

$$\rho(\mathbf{H}) = \|\mathbf{U}_{\mathbf{x}^*}(\mathbf{I}_d - \eta\mathbf{U}_{\mathbf{x}^*}^\top\mathbf{A}^\top\mathbf{A}\mathbf{U}_{\mathbf{x}^*})\mathbf{U}_{\mathbf{x}^*}^\top\|_2.$$

Using the fact that the spectral norm is invariant under left-multiplication by matrices with orthonormal columns and right-multiplication by matrices with orthonormal rows (see [58] - Exercise 5.6.9), we further have

$$\rho(\mathbf{H}) = \|\mathbf{I}_d - \eta\mathbf{U}_{\mathbf{x}^*}^\top\mathbf{A}^\top\mathbf{A}\mathbf{U}_{\mathbf{x}^*}\|_2. \quad (76)$$

Let  $\mathbf{U}_{\mathbf{x}^*}^\top\mathbf{A}^\top\mathbf{A}\mathbf{U}_{\mathbf{x}^*} = \hat{\mathbf{U}}\hat{\mathbf{\Lambda}}\hat{\mathbf{U}}^\top$  be an eigendecomposition, where  $\hat{\mathbf{U}} \in \mathbb{R}^{d \times d}$  is an orthogonal matrix and  $\hat{\mathbf{\Lambda}} = \text{diag}(\lambda_1(\mathbf{U}_{\mathbf{x}^*}^\top\mathbf{A}^\top\mathbf{A}\mathbf{U}_{\mathbf{x}^*}), \dots, \lambda_d(\mathbf{U}_{\mathbf{x}^*}^\top\mathbf{A}^\top\mathbf{A}\mathbf{U}_{\mathbf{x}^*}))$ . Since  $\hat{\mathbf{U}}^\top\hat{\mathbf{U}} = \mathbf{I}_d$ , (76) can be represented as

$$\begin{aligned} \rho(\mathbf{H}) &= \left\| \hat{\mathbf{U}}(\mathbf{I}_d - \eta\hat{\mathbf{\Lambda}})\hat{\mathbf{U}}^\top \right\|_2 \\ &= \left\| \mathbf{I}_d - \eta\hat{\mathbf{\Lambda}} \right\|_2. \end{aligned}$$

Now using the fact that the spectral norm of a diagonal matrix is the maximum of the absolute values of its diagonal entries, we obtain

$$\begin{aligned} \rho(\mathbf{H}) &= \max_{1 \leq i \leq d} |1 - \eta\lambda_i(\mathbf{U}_{\mathbf{x}^*}^\top\mathbf{A}^\top\mathbf{A}\mathbf{U}_{\mathbf{x}^*})| \\ &= \max\{|1 - \eta\lambda_1|, |1 - \eta\lambda_d|\}. \end{aligned}$$

Second, we establish the sufficient conditions for  $\rho(\mathbf{H}) < 1$  by bounding each term inside the maximum in (18) as follows. Since  $\lambda_d \geq 0$ , we have

$$-1 < 1 - \eta\lambda_1 \leq 1 - \eta\lambda_d \leq 1, \text{ for } i = 1, \dots, d,$$

if  $0 < \eta < 2/\lambda_1$ . It is also noted from the definition of the spectral norm that  $\|\mathbf{A}\mathbf{U}_{\mathbf{x}^*}\|_2^2 = \lambda_1$ . Therefore,  $\rho(\mathbf{H}) \leq 1$  provided that (17) holds. The equality  $\rho(\mathbf{H}) = 1$  holds if and only if  $\lambda_d = 0$ , i.e.,  $(\mathbf{A}\mathbf{U}_{\mathbf{x}^*})^\top\mathbf{A}\mathbf{U}_{\mathbf{x}^*}$  is singular. In other words, when  $(\mathbf{A}\mathbf{U}_{\mathbf{x}^*})^\top\mathbf{A}\mathbf{U}_{\mathbf{x}^*}$  is full rank and (17) holds, the linear convergence is guaranteed as  $\rho(\mathbf{H}) < 1$ .

Finally, the region of linear convergence in (19) is determined based on simplifying (12) as follows. First, using Remark 1, we obtain  $\kappa(\mathbf{Q}) = 1$ . Second, from (16), we have  $\|\nabla\mathcal{P}_C(\mathbf{z}_\eta^*)\|_2 = \|\mathcal{P}_{T_{\mathbf{x}^*}(C)}\|_2 = 1$ . Third, substituting  $\kappa(\mathbf{Q}) = 1$  and  $\|\nabla\mathcal{P}_C(\mathbf{z}_\eta^*)\|_2 = 1$  into (12) yields (19). This completes our proof of the lemma.

#### APPENDIX D PROOF OF LEMMA 2

Our goal is to show the error vector  $\delta^{(k)}$  satisfies the asymptotically-linear quadratic system dynamic in (24) and to bound the norm of the residual  $\mathbf{q}_2$  by (25).

First, our key idea in proving (24) is the Lipschitz-continuous differentiability of  $\mathcal{P}_C$  at  $\mathbf{x}^*$  and at  $\mathbf{z}_\eta^*$ . Specifically, for any  $k$  such that  $\delta^{(k)}$  admits a perturbation  $(\mathbf{I} - \eta\mathbf{A}^\top\mathbf{A})\delta^{(k)}$  that satisfies

$$\|(\mathbf{I} - \eta\mathbf{A}^\top\mathbf{A})\delta^{(k)}\| < c_1(\mathbf{z}_\eta^*), \quad (77)$$

applying the Lipschitz-continuous differentiability of  $\mathcal{P}_C$  at  $\mathbf{z}_\eta^*$  to (22) yields

$$\delta^{(k+1)} = \nabla\mathcal{P}_C(\mathbf{z}_\eta^*)(\mathbf{I} - \eta\mathbf{A}^\top\mathbf{A})\delta^{(k)} + \mathbf{q}_1(\delta^{(k)}), \quad (78)$$

where the residual  $\mathbf{q}_1 : \mathbb{R}^n \rightarrow \mathbb{R}^n$  satisfies

$$\begin{aligned} \|\mathbf{q}_1(\delta^{(k)})\| &\leq c_2(\mathbf{z}_\eta^*)\|(\mathbf{I} - \eta\mathbf{A}^\top\mathbf{A})\delta^{(k)}\|^2 \\ &\leq c_2(\mathbf{z}_\eta^*)u_\eta^2\|\delta^{(k)}\|^2. \end{aligned} \quad (79)$$

On the other hand, using the fact that  $\mathbf{x}^* = \mathcal{P}_C(\mathbf{x}^*)$ ,  $\mathbf{x}^{(k)} = \mathcal{P}_C(\mathbf{x}^{(k)})$ , and the Lipschitz-continuous differentiability of  $\mathcal{P}_C$  at  $\mathbf{x}^*$  with the perturbation  $\delta^{(k)} \in \mathcal{B}(\mathbf{0}, c_1(\mathbf{x}^*))$ , we obtain

$$\begin{aligned} \delta^{(k)} &= \mathbf{x}^{(k)} - \mathbf{x}^* \\ &= \mathcal{P}_C(\mathbf{x}^* + \delta^{(k)}) - \mathcal{P}_C(\mathbf{x}^*) \\ &= \nabla\mathcal{P}_C(\mathbf{x}^*)\delta^{(k)} + \mathbf{q}_{\mathbf{x}^*}(\delta^{(k)}), \end{aligned} \quad (80)$$

where the residual  $\mathbf{q}_{\mathbf{x}^*} : \mathbb{R}^n \rightarrow \mathbb{R}^n$  satisfies  $\|\mathbf{q}_{\mathbf{x}^*}(\delta^{(k)})\| \leq c_2(\mathbf{x}^*)\|\delta^{(k)}\|^2$ . We proceed with the proof of (24) by combining the results from (78) and (80) as follows. Since  $\|(\mathbf{I} - \eta\mathbf{A}^\top\mathbf{A})\delta^{(k)}\| \leq \|\mathbf{I} - \eta\mathbf{A}^\top\mathbf{A}\|_2 \cdot \|\delta^{(k)}\| = u_\eta\|\delta^{(k)}\|$ , the sufficient condition for (77) is  $\|\delta^{(k)}\| < c_1(\mathbf{z}_\eta^*)/u_\eta$ . Thus,  $\|\delta^{(k)}\| < \min\{c_1(\mathbf{x}^*), c_1(\mathbf{z}_\eta^*)/u_\eta\}$  is sufficient for both (78) and (80). Substituting (80) into the RHS of (78), we obtain (24) with

$$\mathbf{q}_2(\delta^{(k)}) = \nabla\mathcal{P}_C(\mathbf{z}_\eta^*)(\mathbf{I} - \eta\mathbf{A}^\top\mathbf{A})\mathbf{q}_{\mathbf{x}^*}(\delta^{(k)}) + \mathbf{q}_1(\delta^{(k)}). \quad (81)$$

Next, to bound the norm of the residual  $\mathbf{q}_2$ , we take the norm of both sides of (81) and apply the triangle inequality as follows

$$\begin{aligned} \|\mathbf{q}_2(\delta^{(k)})\| &\leq \|\nabla\mathcal{P}_C(\mathbf{z}_\eta^*)(\mathbf{I} - \eta\mathbf{A}^\top\mathbf{A})\mathbf{q}_{\mathbf{x}^*}(\delta^{(k)})\| \\ &\quad + \|\mathbf{q}_1(\delta^{(k)})\|. \end{aligned} \quad (82)$$

On the one hand, the first term on the RHS of (82) can be bounded by

$$\begin{aligned} & \|\nabla\mathcal{P}_C(\mathbf{z}_\eta^*) \cdot (\mathbf{I} - \eta\mathbf{A}^\top\mathbf{A})\mathbf{q}_{\mathbf{x}^*}(\boldsymbol{\delta}^{(k)})\| \\ & \leq \|\nabla\mathcal{P}_C(\mathbf{z}_\eta^*)\|_2 \cdot \|\mathbf{I} - \eta\mathbf{A}^\top\mathbf{A}\|_2 \cdot \|\mathbf{q}_{\mathbf{x}^*}(\boldsymbol{\delta}^{(k)})\| \\ & \leq \|\nabla\mathcal{P}_C(\mathbf{z}_\eta^*)\|_2 \cdot u_\eta \cdot c_2(\mathbf{x}^*) \|\boldsymbol{\delta}^{(k)}\|^2. \end{aligned} \quad (83)$$

On the other hand, the second term on the RHS of (82) can be bounded by (79). Therefore, combining the two bounds, we obtain (25).

#### APPENDIX E PROOF OF LEMMA 3

In this section, our goal is to show the recursion on the transformed error vector (28) holds at any  $k \in \mathbb{N}$  provided that the initial error vector lies within the region of linear convergence described by (12). In the first step, we prove that if the current transformed error vector lies within the region of linear convergence

$$\|\tilde{\boldsymbol{\delta}}^{(k)}\| < \min\left\{\frac{c_1(\mathbf{x}^*)}{\|\mathbf{Q}\|_2}, \frac{c_1(\mathbf{z}_\eta^*)}{\|\mathbf{Q}\|_2 u_\eta}, \frac{1 - \rho(\mathbf{H})}{q/\|\mathbf{Q}^{-1}\|_2}\right\}. \quad (84)$$

then  $\tilde{\boldsymbol{\delta}}^{(k+1)} = \boldsymbol{\Lambda}\tilde{\boldsymbol{\delta}}^{(k)} + \mathbf{q}_3(\tilde{\boldsymbol{\delta}}^{(k)})$  and moreover, the next transformed error vector also lies within the region of linear convergence

$$\|\tilde{\boldsymbol{\delta}}^{(k+1)}\| < \min\left\{\frac{c_1(\mathbf{x}^*)}{\|\mathbf{Q}\|_2}, \frac{c_1(\mathbf{z}_\eta^*)}{\|\mathbf{Q}\|_2 u_\eta}, \frac{1 - \rho(\mathbf{H})}{q/\|\mathbf{Q}^{-1}\|_2}\right\}. \quad (85)$$

Therefore, by the principle of induction, the initial condition on the transformed error vector, i.e., (84) holds at  $k = 0$ , is the sufficient condition for (28) to hold at any  $k \in \mathbb{N}$ . In the second step, we show that (84) holds at  $k = 0$  if the initial condition on the error vector (12) holds and hence, completes the proof of lemma. We proceed with our detailed proof below.

First, let us assume that (84) holds. We have

$$\begin{aligned} \|\boldsymbol{\delta}^{(k)}\| & = \|\mathbf{Q}\tilde{\boldsymbol{\delta}}^{(k)}\| \\ & \leq \|\mathbf{Q}\|_2 \|\tilde{\boldsymbol{\delta}}^{(k)}\| \\ & < \|\mathbf{Q}\|_2 \cdot \min\left\{\frac{c_1(\mathbf{x}^*)}{\|\mathbf{Q}\|_2}, \frac{c_1(\mathbf{z}_\eta^*)}{\|\mathbf{Q}\|_2 u_\eta}, \frac{1 - \rho(\mathbf{H})}{q/\|\mathbf{Q}^{-1}\|_2}\right\} \\ & \leq \min\left\{c_1(\mathbf{x}^*), \frac{c_1(\mathbf{z}_\eta^*)}{u_\eta}\right\}, \end{aligned} \quad (86)$$

Thus, by Lemma 2, we have  $\boldsymbol{\delta}^{(k+1)} = \mathbf{H}\boldsymbol{\delta}^{(k)} + \mathbf{q}_2(\boldsymbol{\delta}^{(k)})$ . Substituting  $\mathbf{H} = \mathbf{Q}\boldsymbol{\Lambda}\mathbf{Q}^{-1}$  and multiplying both sides with  $\mathbf{Q}^{-1}$  yields

$$\mathbf{Q}^{-1}\boldsymbol{\delta}^{(k+1)} = \boldsymbol{\Lambda}\mathbf{Q}^{-1}\boldsymbol{\delta}^{(k)} + \mathbf{Q}^{-1}\mathbf{q}_2(\boldsymbol{\delta}^{(k)}).$$

Replacing  $\mathbf{Q}^{-1}\boldsymbol{\delta}^{(k)}$  by  $\tilde{\boldsymbol{\delta}}^{(k)}$  and  $\boldsymbol{\delta}^{(k)}$  by  $\mathbf{Q}\tilde{\boldsymbol{\delta}}^{(k)}$  in the last equation, we obtain (28), i.e.,  $\tilde{\boldsymbol{\delta}}^{(k+1)} = \boldsymbol{\Lambda}\tilde{\boldsymbol{\delta}}^{(k)} + \mathbf{q}_3(\tilde{\boldsymbol{\delta}}^{(k)})$ . Here, the second term  $\mathbf{q}_3$  can be bounded as follows

$$\begin{aligned} \|\mathbf{q}_3(\tilde{\boldsymbol{\delta}}^{(k)})\| & = \|\mathbf{Q}^{-1}\mathbf{q}_2(\mathbf{Q}\tilde{\boldsymbol{\delta}}^{(k)})\| \\ & \leq \|\mathbf{Q}^{-1}\|_2 \|\mathbf{q}_2(\mathbf{Q}\tilde{\boldsymbol{\delta}}^{(k)})\| \\ & \leq \|\mathbf{Q}^{-1}\|_2 (c_2(\mathbf{x}^*) + \|\nabla\mathcal{P}_C(\mathbf{z}_\eta^*)\|_2 c_2(\mathbf{z}_\eta^*)) \|\mathbf{Q}\tilde{\boldsymbol{\delta}}^{(k)}\|^2 \\ & \leq \|\mathbf{Q}^{-1}\|_2 (c_2(\mathbf{x}^*) + \|\nabla\mathcal{P}_C(\mathbf{z}_\eta^*)\|_2 c_2(\mathbf{z}_\eta^*)) \|\mathbf{Q}\|_2^2 \|\tilde{\boldsymbol{\delta}}^{(k)}\|^2 \\ & = \frac{q}{\|\mathbf{Q}^{-1}\|_2} \|\tilde{\boldsymbol{\delta}}^{(k)}\|^2. \end{aligned} \quad (87)$$

Now, taking the norms of both sides of (28) and applying the triangle inequality yield

$$\begin{aligned} \|\tilde{\boldsymbol{\delta}}^{(k+1)}\| & \leq \|\boldsymbol{\Lambda}\tilde{\boldsymbol{\delta}}^{(k)}\| + \|\mathbf{q}_3(\tilde{\boldsymbol{\delta}}^{(k)})\| \\ & \leq \rho(\mathbf{H})\|\tilde{\boldsymbol{\delta}}^{(k)}\| + \frac{q}{\|\mathbf{Q}^{-1}\|_2} \|\tilde{\boldsymbol{\delta}}^{(k)}\|^2 \\ & < \rho(\mathbf{H})\|\tilde{\boldsymbol{\delta}}^{(k)}\| + (1 - \rho(\mathbf{H}))\|\tilde{\boldsymbol{\delta}}^{(k)}\| \\ & = \|\tilde{\boldsymbol{\delta}}^{(k)}\|, \end{aligned} \quad (88)$$

where the second inequality stems from  $\|\tilde{\boldsymbol{\delta}}^{(k)}\| < (1 - \rho(\mathbf{H})) / (q/\|\mathbf{Q}^{-1}\|_2)$ . From (84) and (88), we conclude that (85) holds. By the principle of induction, we have (84) holds for all  $k \in \mathbb{N}$  provided that it holds at  $k = 0$ , i.e.,

$$\|\tilde{\boldsymbol{\delta}}^{(0)}\| < \min\left\{\frac{c_1(\mathbf{x}^*)}{\|\mathbf{Q}\|_2}, \frac{c_1(\mathbf{z}_\eta^*)}{\|\mathbf{Q}\|_2 u_\eta}, \frac{1 - \rho(\mathbf{H})}{q/\|\mathbf{Q}^{-1}\|_2}\right\}. \quad (89)$$

Second, we prove that (12) is sufficient for (89). Using the definition  $\tilde{\boldsymbol{\delta}}^{(k)} = \mathbf{Q}^{-1}\boldsymbol{\delta}^{(k)}$ , we have

$$\|\tilde{\boldsymbol{\delta}}^{(k)}\| = \|\mathbf{Q}^{-1}\boldsymbol{\delta}^{(k)}\| \leq \|\mathbf{Q}^{-1}\|_2 \|\boldsymbol{\delta}^{(k)}\|. \quad (90)$$

Upper-bounding  $\|\boldsymbol{\delta}^{(k)}\|$  by the LHS of (12) and substituting back into (90) yield

$$\|\tilde{\boldsymbol{\delta}}^{(k)}\| < \|\mathbf{Q}^{-1}\|_2 \cdot \min\left\{\frac{c_1(\mathbf{x}^*)}{\kappa(\mathbf{Q})}, \frac{c_1(\mathbf{z}_\eta^*)}{\kappa(\mathbf{Q})u_\eta}, \frac{1 - \rho(\mathbf{H})}{q}\right\}.$$

Finally, replacing  $\kappa(\mathbf{Q})$  by the product  $\|\mathbf{Q}\|_2 \cdot \|\mathbf{Q}^{-1}\|_2$  and simplifying yield (89). This completes our proof of the lemma.

#### APPENDIX F PROOF OF LEMMA 4

In this section, we show the convergence of  $\{\|\tilde{\boldsymbol{\delta}}^{(k)}\|\}_{k=0}^\infty$  using Theorem 1 in [49]. Our idea is to consider a surrogate sequence  $\{a_k\}_{k=0}^\infty$  that upper-bounds  $\{\|\tilde{\boldsymbol{\delta}}^{(k)}\|\}_{k=0}^\infty$ :

$$\begin{cases} a_0 = \|\tilde{\boldsymbol{\delta}}^{(0)}\|, \\ a_{k+1} = \rho(\mathbf{H})a_k + \frac{q}{\|\mathbf{Q}^{-1}\|_2} a_k^2. \end{cases}$$

First, we prove by induction that

$$\|\tilde{\boldsymbol{\delta}}^{(k)}\| \leq a_k \quad \forall k \in \mathbb{N}. \quad (91)$$

The base case when  $k = 0$  holds trivially as  $a_0 = \|\tilde{\boldsymbol{\delta}}^{(0)}\|$ . In the induction step, given  $\|\tilde{\boldsymbol{\delta}}^{(k)}\| \leq a_k$  for some integer  $k \geq 0$ , we have

$$\begin{aligned} \|\tilde{\boldsymbol{\delta}}^{(k+1)}\| & \leq \rho(\mathbf{H})\|\tilde{\boldsymbol{\delta}}^{(k)}\| + \frac{q}{\|\mathbf{Q}^{-1}\|_2} \|\tilde{\boldsymbol{\delta}}^{(k)}\|^2 \\ & \leq \rho a_k + \frac{q}{\|\mathbf{Q}^{-1}\|_2} a_k^2 = a_{k+1}. \end{aligned}$$

By the principle of induction, (91) holds for all  $k \in \mathbb{N}$ . Next, applying Theorem 1 in [49], under the condition  $a_0 = \|\tilde{\boldsymbol{\delta}}^{(0)}\| < (1 - \rho(\mathbf{H})) / (q/\|\mathbf{Q}^{-1}\|_2)$ , yields  $a_k \leq \tilde{a}_0$  for any integer  $k$  satisfies (30). From (91), we further have  $\|\tilde{\boldsymbol{\delta}}^{(k)}\| \leq a_k \leq \tilde{a}_0 = \tilde{\epsilon}\|\tilde{\boldsymbol{\delta}}^{(0)}\|$ . This completes our proof of the lemma.

APPENDIX G  
DETAILS OF APPLICATION B - ITERATIVE HARD  
THRESHOLDING FOR SPARSE RECOVERY

A. Proof of (41)

In this subsection, we first show that any  $\mathbf{x}^* \in \Phi_{=s}$  and  $\mathbf{x} \in \mathcal{B}(\mathbf{x}^*, |x_{[s]}^*|/\sqrt{2})$  share the same index set of  $s$ -largest elements (in magnitude), i.e.,  $\Omega_s(\mathbf{x}^*)$ . Then, we construct a counter-example to demonstrate that  $|x_{[s]}^*|/\sqrt{2}$  is the largest possible radius so that (41) holds.

First, we show that for any  $i \in \Omega_s(\mathbf{x}^*)$  and  $j \in \{1, \dots, n\} \setminus \Omega_s(\mathbf{x}^*)$ ,  $|x_j| < |x_i|$  as follows. In particular, we have

$$\begin{aligned} |x_j - x_j^*| + |x_i - x_i^*| &\leq \sqrt{2((x_j - x_{[j]}^*)^2 + (x_i - x_i^*)^2)} \\ &\leq \sqrt{2\|\mathbf{x} - \mathbf{x}^*\|^2} \\ &< |x_{[s]}^*|, \end{aligned}$$

where the last inequality stems from the fact that  $\|\mathbf{x} - \mathbf{x}^*\| < |x_{[s]}^*|/\sqrt{2}$ . Now, since  $x_j^* = 0$  for all  $j \in \{1, \dots, n\} \setminus \Omega_s(\mathbf{x}^*)$ , we have

$$\begin{aligned} |x_j| &= |x_j - x_j^*| \\ &< |x_{[s]}^*| - |x_i - x_i^*| \\ &\leq |x_i^*| - |x_i - x_i^*| \\ &\leq |x_i^*| + (x_i - x_i^*) = |x_i|, \end{aligned} \quad (92)$$

Therefore, every  $\mathbf{x} \in \mathcal{B}(\mathbf{x}^*, |x_{[s]}^*|/\sqrt{2})$  shares the same index set of  $s$ -largest (in magnitude) elements with  $\mathbf{x}^*$ , i.e.,  $\Omega_s(\mathbf{x}) = \Omega_s(\mathbf{x}^*)$ , which implies (41).

We now construct the counter-example as a point  $\mathbf{x}$  such that  $\Omega_s(\mathbf{x}) \neq \Omega_s(\mathbf{x}^*)$  and  $\mathbf{x}$  is not in  $\mathcal{B}(\mathbf{x}^*, |x_{[s]}^*|/\sqrt{2})$  but arbitrarily close to its boundary. Without loss of generality, assume that  $|x_1^*| \geq \dots \geq |x_s^*| > |x_{s+1}^*| = \dots = |x_n^*| = 0$ . For arbitrarily small  $\epsilon > 0$ , define  $\mathbf{x}$  as

$$x_i = \begin{cases} x_s^*/2 & \text{if } i = s, \\ x_s^*/2 + \epsilon & \text{if } i = s + 1, \\ x_i & \text{otherwise.} \end{cases}$$

Then, since  $x_{s+1} < x_s$ ,  $\mathbf{x}$  does not share the same index set of  $s$ -largest (in magnitude) elements with  $\mathbf{x}^*$ . On the other hand, as  $\epsilon \rightarrow 0$ , we have

$$\begin{aligned} \|\mathbf{x} - \mathbf{x}^*\| &= \sqrt{\sum_{i=1}^n (x_i - x_i^*)^2} \\ &= \sqrt{\left(-\frac{x_s^*}{2}\right)^2 + \left(\frac{x_s^*}{2} + \epsilon\right)^2} \rightarrow \frac{1}{\sqrt{2}}|x_{[s]}^*|. \end{aligned}$$

This means  $\mathbf{x} \notin \mathcal{B}(\mathbf{x}^*, |x_{[s]}^*|/\sqrt{2})$  but it can approach the boundary of the ball as  $\epsilon$  decreases to 0.

B. Proof of Remark 5

In the following, we show any stationary point  $\mathbf{x}^*$  of (39) is also a local minimum by proving that the objective function does not decrease if we add any perturbation to  $\mathbf{x}^*$  on  $\Phi_{\leq s}$ . Let us consider any perturbation  $\delta$  such that  $\delta \in \mathcal{B}(\mathbf{0}, c_1(\mathbf{x}^*))$  and  $\mathbf{x} = \mathbf{x}^* + \delta \in \Phi_{\leq s}$ . Since  $\mathbf{x} \in \mathcal{B}(\mathbf{x}^*, c_1(\mathbf{x}^*))$ , using (92), we have  $|x_{[1]}| \geq \dots |x_{[s]}| > 0$ . On the other hand, since

$\mathbf{x} \in \Phi_{\leq s}$ , it must hold that  $|x_{[s+1]}| = \dots = |x_{[n]}| = 0$ . Therefore,  $\mathbf{x} = \mathbf{S}_{\mathbf{x}^*} \mathbf{S}_{\mathbf{x}^*}^\top \mathbf{x}$ , which implies  $\delta = \mathbf{S}_{\mathbf{x}^*} \mathbf{S}_{\mathbf{x}^*}^\top \delta$ . Now we represent the change in the objective function as

$$\begin{aligned} &\frac{1}{2}\|\mathbf{A}(\mathbf{x}^* + \delta) - \mathbf{b}\|^2 - \frac{1}{2}\|\mathbf{A}\mathbf{x}^* - \mathbf{b}\|^2 \\ &= \frac{1}{2}\delta^\top \mathbf{A}^\top \mathbf{A} \delta + \delta^\top \mathbf{A}^\top (\mathbf{A}\mathbf{x}^* - \mathbf{b}) \\ &= \frac{1}{2}\delta^\top \mathbf{S}_{\mathbf{x}^*} \mathbf{S}_{\mathbf{x}^*}^\top \mathbf{A}^\top \mathbf{A} \mathbf{S}_{\mathbf{x}^*} \mathbf{S}_{\mathbf{x}^*}^\top \delta + \delta^\top \mathbf{S}_{\mathbf{x}^*} \mathbf{S}_{\mathbf{x}^*}^\top \mathbf{A}^\top (\mathbf{A}\mathbf{x}^* - \mathbf{b}) \\ &= \frac{1}{2}\delta^\top \mathbf{S}_{\mathbf{x}^*} (\mathbf{S}_{\mathbf{x}^*}^\top \mathbf{A}^\top \mathbf{A} \mathbf{S}_{\mathbf{x}^*}) \mathbf{S}_{\mathbf{x}^*}^\top \delta \geq 0, \end{aligned} \quad (93)$$

where the last equality uses the stationarity condition in (42). From (93), we conclude  $\mathbf{x}^*$  is a local minimum of (39).

REFERENCES

- [1] M. A. Figueiredo, R. D. Nowak, and S. J. Wright, "Gradient projection for sparse reconstruction: Application to compressed sensing and other inverse problems," *IEEE J. Sel. Top. Signal. Process.*, vol. 1, no. 4, pp. 586–597, 2007.
- [2] T. Blumensath and M. E. Davies, "Iterative thresholding for sparse approximations," *J. Fourier Anal. Appl.*, vol. 14, no. 5-6, pp. 629–654, 2008.
- [3] —, "Iterative hard thresholding for compressed sensing," *Appl. Comput. Harmon. Anal.*, vol. 27, no. 3, pp. 265–274, 2009.
- [4] B. R. Hunt, "The application of constrained least squares estimation to image restoration by digital computer," *IEEE Trans. Comput.*, vol. 100, no. 9, pp. 805–812, 1973.
- [5] N. P. Galatsanos, A. K. Katsaggelos, R. T. Chin, and A. D. Hillery, "Least squares restoration of multichannel images," *IEEE Trans. Signal Process.*, vol. 39, no. 10, pp. 2222–2236, 1991.
- [6] V. Z. Mesarovic, N. P. Galatsanos, and A. K. Katsaggelos, "Regularized constrained total least squares image restoration," *IEEE Trans. Image Process.*, vol. 4, no. 8, pp. 1096–1108, 1995.
- [7] C. I. Puryear, O. N. Portniaguine, C. M. Cobos, and J. P. Castagna, "Constrained least-squares spectral analysis: Application to seismic data," *Geophysics*, vol. 77, no. 5, pp. V143–V167, 2012.
- [8] Y. Chen, J. Yuan, S. Zu, S. Qu, and S. Gan, "Seismic imaging of simultaneous-source data using constrained least-squares reverse time migration," *J. Appl. Geophys.*, vol. 114, pp. 32–35, 2015.
- [9] W. Menke, *Geophysical data analysis: Discrete inverse theory*. Academic press, 2018.
- [10] J. Tranter, N. D. Sidiropoulos, X. Fu, and A. Swami, "Fast unit-modulus least squares with applications in beamforming," *IEEE Trans. Signal Process.*, vol. 65, no. 11, pp. 2875–2887, 2017.
- [11] M. Zhang, J. Li, S. Zhu, and X. Chen, "Fast and simple gradient projection algorithms for phase-only beamforming," *IEEE Trans. Veh. Technol.*, 2021.
- [12] P. Jain, R. Meka, and I. S. Dhillon, "Guaranteed rank minimization via singular value projection," in *Proc. Adv. Neural Inf. Process. Syst.*, 2010, pp. 937–945.
- [13] Y. Chen and M. J. Wainwright, "Fast low-rank estimation by projected gradient descent: General statistical and algorithmic guarantees," *arXiv preprint arXiv:1509.03025*, 2015.
- [14] R. Khanna and A. Kyrillidis, "IHT dies hard: Provable accelerated iterative hard thresholding," in *Proc. Int. Conf. Artif. Intell. Stat.*, 2018, pp. 188–198.
- [15] C.-J. Lin, "Projected gradient methods for nonnegative matrix factorization," *Neural Comput.*, vol. 19, no. 10, pp. 2756–2779, 2007.
- [16] N. Mohammadiha and A. Leijon, "Nonnegative matrix factorization using projected gradient algorithms with sparseness constraints," in *IEEE Int. Symp. Signal Process. Inf. Technol.* IEEE, 2009, pp. 418–423.
- [17] N. Guan, D. Tao, Z. Luo, and B. Yuan, "NeNMF: An optimal gradient method for nonnegative matrix factorization," *IEEE Trans. Signal Process.*, vol. 60, no. 6, pp. 2882–2898, 2012.
- [18] D. G. Luenberger, Y. Ye *et al.*, *Linear and nonlinear programming*. Springer, 1984, vol. 2.
- [19] D. P. Bertsekas, "Nonlinear programming," *J. Oper. Res. Soc.*, vol. 48, no. 3, pp. 334–334, 1997.
- [20] A. Beck, *First-order methods in optimization*. SIAM, 2017.
- [21] P. Jain, P. Kar *et al.*, "Non-convex optimization for machine learning," *Found. Trends Mach. Learn.*, vol. 10, no. 3-4, pp. 142–336, 2017.

- [22] P. L. Combettes and J.-C. Pesquet, "Proximal splitting methods in signal processing," in *Fixed-point algorithms for inverse problems in science and engineering*. Springer, 2011, pp. 185–212.
- [23] E. J. Candes and T. Tao, "Decoding by linear programming," *IEEE Trans. Inf. Theory*, vol. 51, no. 12, pp. 4203–4215, 2005.
- [24] R. Sun and Z.-Q. Luo, "Guaranteed matrix completion via non-convex factorization," *IEEE Trans. Inf. Theory*, vol. 62, no. 11, pp. 6535–6579, 2016.
- [25] A. Beck and Y. Vaisbourd, "Globally solving the trust region subproblem using simple first-order methods," *SIAM J. Optim.*, vol. 28, no. 3, pp. 1951–1967, 2018.
- [26] D. G. Luenberger, "The gradient projection method along geodesics," *Manag. Sci.*, vol. 18, no. 11, pp. 620–631, 1972.
- [27] A. Lichnewsky, "Minimisation des fonctionnelles définies sur une variété par la méthode du gradient conjugué," Ph.D. dissertation, Thèse de Doctorat d'Etat. Paris: Université de Paris-Sud, 1979.
- [28] D. Gabay, "Minimizing a differentiable function over a differential manifold," *J. Optim. Theory Appl.*, vol. 37, no. 2, pp. 177–219, 1982.
- [29] A. Uschmajew and B. Vandereycken, "Geometric methods on low-rank matrix and tensor manifolds," in *Variational methods for nonlinear geometric data and applications*. Springer Nature, 2020, pp. 261–313.
- [30] B. O'donoghue and E. Candes, "Adaptive restart for accelerated gradient schemes," *Found. Comput. Math.*, vol. 15, no. 3, pp. 715–732, 2015.
- [31] W. G. Strang, "On the kantorovich inequality," in *Proc. Amer. Math. Soc.*, vol. 11, no. 468, 1960, pp. 0095–09 601.
- [32] E. Chunikhina, R. Raich, and T. Nguyen, "Performance analysis for matrix completion via iterative hard-thresholded SVD," in *Proc. IEEE Stat. Signal Process. Workshop*. IEEE, 2014, pp. 392–395.
- [33] T. Vu and R. Raich, "Accelerating iterative hard thresholding for low-rank matrix completion via adaptive restart," in *Proc. IEEE Int. Conf. Acoust. Speech Signal Process.* IEEE, 2019, pp. 2917–2921.
- [34] —, "Local convergence of the Heavy Ball method in iterative hard thresholding for low-rank matrix completion," in *Proc. IEEE Int. Conf. Acoust. Speech Signal Process.* IEEE, 2019, pp. 3417–3421.
- [35] T. Vu, R. Raich, and X. Fu, "On convergence of projected gradient descent for minimizing a large-scale quadratic over the unit sphere," in *Proc. IEEE Int. Workshop Mach. Learn. Signal Process.* IEEE, 2019, pp. 1–6.
- [36] T. Vu and R. Raich, "Exact linear convergence rate analysis for low-rank symmetric matrix completion via gradient descent," in *Proc. IEEE Int. Conf. Acoust. Speech Signal Process.* IEEE, 2021, pp. 3240–3244.
- [37] I. Gelfand, "Normierte ringe," *Rec. Math. [Mat. Sbornik]*, vol. 9, no. 1, pp. 3–24, 1941.
- [38] F. Vasilyev and A. Y. Ivanitskiy, *In-depth analysis of linear programming*. Springer Science & Business Media, 2013.
- [39] R. L. Foote, "Regularity of the distance function," *Proc. Am. Math. Soc.*, vol. 92, no. 1, pp. 153–155, 1984.
- [40] E. Dudek and K. Holly, "Nonlinear orthogonal projection," *Ann. Pol. Math.*, vol. 59, no. 1, pp. 1–31, 1994.
- [41] A. S. Lewis and J. Malick, "Alternating projections on manifolds," *Math. Oper. Res.*, vol. 33, no. 1, pp. 216–234, 2008.
- [42] L. Ambrosio and C. Mantegazza, "Curvature and distance function from a manifold," *J. Geom. Anal.*, vol. 8, no. 5, pp. 723–748, 1998.
- [43] P.-A. Absil and J. Malick, "Projection-like retractions on matrix manifolds," *SIAM J. Optim.*, vol. 22, no. 1, pp. 135–158, 2012.
- [44] J. Rataj and M. Zähle, *Curvature measures of singular sets*. Springer, 2019.
- [45] G. Leobacher and A. Steinicke, "Existence, uniqueness and regularity of the projection onto differentiable manifolds," *Ann. Glob. Anal. Geom.*, pp. 1–29, 2021.
- [46] P.-A. Absil, R. Mahony, and R. Sepulchre, *Optimization algorithms on matrix manifolds*. Princeton University Press, 2009.
- [47] B. T. Polyak, *Introduction to optimization. Optimization software*. Inc., Publications Division, New York, 1987, vol. 1.
- [48] S.-G. Hwang, "Cauchy's interlace theorem for eigenvalues of hermitian matrices," *Am. Math. Mon.*, vol. 111, no. 2, pp. 157–159, 2004.
- [49] T. Vu and R. Raich, "A closed-form bound on asymptotic linear convergence of positively quadratic first-order difference equations," *arXiv preprint arXiv:2112.10598*, 2021.
- [50] B. T. Polyak, "Some methods of speeding up the convergence of iteration methods," *USSR Comput. Math. Math. Phys.*, vol. 4, no. 5, pp. 1–17, 1964.
- [51] M. Abramowitz and I. A. Stegun, "Handbook of mathematical functions with formulas, graphs, and mathematical tables," *NBS Appl. Math. Ser.*, vol. 55, 1964.
- [52] L. S. Resende, J. M. T. Romano, and M. G. Bellanger, "A fast least-squares algorithm for linearly constrained adaptive filtering," *IEEE Trans. Signal Process.*, vol. 44, no. 5, pp. 1168–1174, 1996.
- [53] C. Van Loan, "On the method of weighting for equality-constrained least-squares problems," *SIAM J. Numer. Anal.*, vol. 22, no. 5, pp. 851–864, 1985.
- [54] J. C. Dunn, "Global and asymptotic convergence rate estimates for a class of projected gradient processes," *SIAM J. Control Optim.*, vol. 19, no. 3, pp. 368–400, 1981.
- [55] D. P. Bertsekas and E. M. Gafni, "Projection methods for variational inequalities with application to the traffic assignment problem," in *Nondifferential and variational techniques in optimization*. Springer, 1982, pp. 139–159.
- [56] Z.-Q. Luo and P. Tseng, "Error bound and reduced-gradient projection algorithms for convex minimization over a polyhedral set," *SIAM J. Optim.*, vol. 3, no. 1, pp. 43–59, 1993.
- [57] B. Johansson, T. Elfving, V. Kozlov, Y. Censor, P.-E. Forssén, and G. Granlund, "The application of an oblique-projected Landweber method to a model of supervised learning," *Math. comput. model.*, vol. 43, no. 7–8, pp. 892–909, 2006.
- [58] C. D. Meyer, *Matrix analysis and applied linear algebra*. SIAM, 2000, vol. 71.
- [59] A. Tarantola, *Inverse problem theory and methods for model parameter estimation*. SIAM, 2005.
- [60] W. W. Hager, "Minimizing a quadratic over a sphere," *SIAM J. Optim.*, vol. 12, no. 1, pp. 188–208, 2001.
- [61] E. J. Candès and B. Recht, "Exact matrix completion via convex optimization," *Found. Comput. Math.*, vol. 9, no. 6, p. 717, 2009.
- [62] C. Eckart and G. Young, "The approximation of one matrix by another of lower rank," *Psychometrika*, vol. 1, no. 3, pp. 211–218, 1936.
- [63] M. Lee John, "Introduction to smooth manifolds," *Graduate Texts in Mathematics*, vol. 218, 2003.
- [64] T. Vu, E. Chunikhina, and R. Raich, "Perturbation expansions and error bounds for the truncated singular value decomposition," *Linear Algebra Appl.*, 2021.